Interface entangled plasmon-plasmariton modes

Jesper Jung and Ole Keller*
Institute of Physics, Aalborg University, Skjernvej 4A, 9220 Aalborg Øst, Denmark

(Received 19 May 2023; accepted 26 July 2023; published 8 August 2023)

A theoretical study of the propagating electromagnetic surface waves confined to a plane vacuum–homogeneous jellium interface is carried out. A classification of the entangled surface plasmon (L) and plasmariton (T) modes, which we name surface jellions, is given. The collective mode structure is obtained using the Weyl (angular spectrum) expansion of the screened electromagnetic jellium propagator $\mathbf{G}$. The pole structure of $\mathbf{G}$ relates to the collective-mode pattern. The surface jellion dispersion relation is a central concept in our analyses. We derive this for interfaces with and without self-consistently determined surface currents, i.e., for so-called active and passive boundary conditions. A numerical calculation of the dispersion relation is carried out for the hydrodynamic model. For this model the dispersion relation has three branches in the region of strong surface plasmon-plasmariton coupling. Starting from a finite-relaxation time τ calculation, the surface jellion eigenmode structure is obtained in the limit $\tau \rightarrow \infty$. Exponentially confined surface jellion eigenmodes carry electromagnetic momentum along the surface, and we calculate the T, L, and TL parts of the momentum, emphasizing numerical data for the hydrodynamic model. It is shown that the entangled TL part carries a momentum backflow. The energy carried by the confined surface jellions is expressed in terms of an equivalent mass concept. The equivalent mass formulation is useful for a harmonic-oscillator description of the surface jellions and their quantization. The equivalent mass of the three branches of the hydrodynamic jellion dispersion is calculated numerically and the T, L, and TL contributions to the equivalent mass are determined. All numerical calculations presented in the article are carried out as a function of the surface jellion wave number along the surface.

DOI: 10.1103/PhysRevA.108.023507

I. INTRODUCTION

In order to understand numerous aspects of the manner in which incoming electromagnetic fields and electrically charged particles interact with free-electron-like metals and semiconductors on the microscopic level, in a first approximation, theorists often treat the externally induced electron dynamics in the framework of the well-known jellium model [1,2]. In this model the ion potential is smeared out as a uniform background for the conduction-electron motion. Even for jellium the theoretical challenges are formidable. In a certain domain of the field-electron interaction the collective jellium excitations plays a dominant role [3,4], and in this work the focus is on this domain.

The eigenmodes of the collective excitations basically are self-sustaining (running) excitations in the absence of irreversible damping mechanisms. The irreversible damping can be rooted in the jellium's coupling to phonons, magnons, impurities, etc., and in the framework of the jellium approach to single-particle (electron) excitations [5,6]. When the damping mechanisms are weak, the positions of the collective eigenmodes in a frequency–wave-vector diagram signal the condition for resonance excitation in observed spectra [7]. For an (assumed) infinitely extended jellium, running eigenmodes belonging to a given (real) wave vector $\mathbf{q}$ are conveniently divided into two groups with electron displacement parallel (L) and perpendicular (T) to $\mathbf{q}$, respectively. The two types of modes are named bulk plasmon (L) and plasmariton (T) modes. In Sec. IX A we briefly discuss the terminology used for the collective bulk and surface modes in jellium. In the small-wave-number limit ($q \rightarrow 0$) the L and T modes are indistinguishable and with resonance at the (long-wavelength) plasma frequency. The plane-wave T- and L-mode wave-vector spectra form a complete set, and in a sense their great usefulness originates in this and the simplicity of the related polarization displacements.

From an experimental point of view, jellium surfaces are always present and in many cases of indispensable importance for the eigenmode structure (and the observed resonance spectra). Once a surface of a given geometrical structure is introduced, a new kind of eigenmode, called electromagnetic surface waves, appears. In the perhaps simplest case, to which we will limit ourselves, it is assumed that a semi-infinite homogeneous jellium occupies a half space ($z \geqslant 0$), with the rest of space being vacuum. The assumption of homogeneity of the jellium density right up to the surface implies that the electron density variations in the surface region are ignored. These variations originate in the quantum interference between the incoming and specular reflected parts of a plane electron wave function in the assumed sharp ionic step potential (see, e.g., [8,9]). The model underlying this is called the semiclassical infinite-barrier (SCIB) model. The eigenmode analysis for a given wave-vector component along the surface $\mathbf{q}_{\parallel}$ divides

*okeller@physics.aau.dk

into examination of s- and p-polarized fields. In the absence of magnetic permeability only p-polarized eigenmode solutions exist. These eigenmodes are often named surface plasmaritons (see Sec. IX A). In the presence of spatial dispersion both T and L dynamics in the jellium are involved.

In the present article we undertake a systematic study of the surface eigenmode structure based on the so-called Weyl expansion of the electromagnetic field. This expansion dates back to Weyl's paper dealing with the propagation of electromagnetic waves over a conducting sphere [10], where he derived a new representation of a scalar spherical wave field generated by a point source in vacuum. This expansion, also called the angular spectrum expansion, is well known in classical optics when dealing with wave fields in a domain that is either a half space or bounded by two mutually parallel planes [11]. For instance, electromagnetic diffraction from a (small) hole in a plane metallic screen can with advantage be examined starting from the angular spectrum expansion [12].

The Weyl expansion is a two-dimensional (2D) mode representation of a wave field and as such any wave field of our jellium-vacuum half-space system can be synthesized from the surface eigenmodes of the Weyl expansion. We have named these eigenmodes, which in general are interface entangled surface plasmon-plasmariton modes, surface jellions. Our systematic analysis based on the Weyl expansion thus shows the presence of entangled surface plasmon-plasmariton states not appearing in previous studies. We hold the point of view that the surface jellion eigenmodes are the genuine eigenmodes excited in the interaction of incoming electromagnetic waves or charged particles in geometrical configurations well modeled as a semi-infinite jellium-vacuum system.

Our paper is organized as follows. In Sec. II we start from a propagator formalism describing the induced electromagnetics of a spatially dispersive homogeneous jellium. The Weyl integral representation of the propagator has poles in the integrand and the positions of these are related to the plasmariton (T) and plasmon (L) bulk dispersion relation. A residue calculation gives one the propagator form in the pole approximation. The propagator formalism giving the electromagnetic field in space requires a driving current density, which for the eigenmodes must be located in the surface plane and hence closely related to the jump (boundary) conditions for the electromagnetic field. The field associated with the collective jellium modes is studied in Sec. III, and in the wake of a few remarks on bulk jellion eigenmodes in Sec. IV, the central part of our study starts in Sec. V with the establishment of the dispersion relation for surface jellions using in turn so-called passive and active boundary conditions. The whole analysis is based on the SCIB model. In Sec. VI the surface jellion dispersion relation is examined in a hydrodynamic approach, and numerical results are presented for the dispersion relation first for a finite relaxation time τ and then in the eigenmode limit $\tau \to \infty$. It appears that the dispersion relation $\omega = \omega(q_\parallel)$ ($q_\parallel$ being the wave number along the surface) has three branches in a certain $q_\parallel$ range. Outside this range the dispersion relation has two branches, which can be identified as the surface plasmariton and plasmon branches. The presence of three branches is a fingerprint of the plasmon-plasmariton entanglement in the $q_\parallel$ range in which the entanglement is particularly strong. In a certain part of the ω-$q_\parallel$ domain, the field in vacuum and the L and T fields in the jellium all decay exponentially away from the surface plane. Eigenmodes for which this is the case we name confined surface jellion eigenmodes. For these eigenmodes we study the field momentum flow along the surface and present a number of numerical results for the hydrodynamic model, all in Sec. VII. Particular emphasis is put on the momentum backflow which is present in the jellium in the low-wave-number part of the $q_\parallel$ spectrum. In Sec. VIII we discuss the field energy in confined surface jellions. The energy can be described as related to an equivalent surface jellion mass and this equivalent mass connects to a harmonic-oscillator description of the surface jellions. Via the introduction of a set of real canonical coordinate and velocity variables, the harmonic-oscillator Hamiltonian can be quantized in the standard manner. The quantum energy $\hbar\omega_b(q_\parallel)$ obtained from the surface jellion dispersion takes on different values in the three branches ($b = 1, 2, 3$). We finish Sec. VIII with a numerical study of the $q_\parallel$ dependence of the mass $M = M(q_\parallel)$, as this appears in the framework of the hydrodynamic approach. Special attention is devoted to the results for large-$q_\parallel$ values. We conclude our paper in paper in Sec. IX with some remarks and a summary of our results.

II. ELECTRODYNAMICS OF A HOMOGENEOUS JELLIUM IN THE WEYL EXPANSION

A. Spatially dispersive conductivity tensor

In a homogenous infinitely extended (bulk) jellium the linear microscopic conductivity tensor $\boldsymbol{\sigma}(\mathbf{r}, \mathbf{r}', t, t')$ is translationally invariant in both space $\mathbf{r}$ and time t, i.e., $\boldsymbol{\sigma}(\mathbf{r}, \mathbf{r}', t, t') = \boldsymbol{\sigma}(\mathbf{r} - \mathbf{r}', t - t')$. The space-time Fourier integral transform ($\mathbf{R} = \mathbf{r} - \mathbf{r}'$ and $\tau = t - t'$)

$$\boldsymbol{\sigma}(\mathbf{q}, \omega) = \int_{-\infty}^{\infty} \boldsymbol{\sigma}(\mathbf{R}, \tau) e^{-i(\mathbf{q}\cdot\mathbf{R} - \omega\tau)} d^3R\, d\tau, \tag{1}$$

giving the conductivity tensor in the wave-vector ($\mathbf{q}$)–frequency (ω) domain, can, due to the rotational invariance of the jellium, be decomposed as

$$\boldsymbol{\sigma}(\mathbf{q}, \omega) = \sigma_T(q, \omega)(\mathbf{U} - \hat{\mathbf{q}}\hat{\mathbf{q}}) + \sigma_L(q, \omega)\hat{\mathbf{q}}\hat{\mathbf{q}}. \tag{2}$$

In Eq. (2), $\mathbf{U}$ is the 3×3 unit tensor and $\hat{\mathbf{q}} = \mathbf{q}/q$ is a unit vector in the $\mathbf{q}$ direction. The scalar quantities $\sigma_T(q, \omega)$ and $\sigma_L(q, \omega)$ are transverse (T) and longitudinal (L) microscopic conductivities. As indicated, these depend only on the magnitude q of the wave vector (and on the frequency).

B. Propagator function formalism in the (ω, q) domain

In microscopic Maxwell-Lorentz dynamics, the wave equation for the microscopic electric field $\mathbf{E}(\mathbf{r}, t)$ [with Fourier transform $\mathbf{E}(\mathbf{q}, \omega)$] hence takes the well-known form

$$\left\{\left[\left(\frac{\omega}{c}\right)^2 - q^2\right]\mathbf{U} + \mathbf{q}\mathbf{q}\right\} \cdot \mathbf{E}(\mathbf{q}, \omega) = -i\mu_0\omega\mathbf{J}(\mathbf{q}, \omega) \tag{3}$$

in the (ω, $\mathbf{q}$) domain, c being the vacuum speed of light. In the presence of a yet unknown external current density $\mathbf{J}^{\text{ext}}(\mathbf{q}, \omega)$, the total current density is given by

$$\mathbf{J}(\mathbf{q}, \omega) = \boldsymbol{\sigma}(\mathbf{q}, \omega) \cdot \mathbf{E}(\mathbf{q}, \omega) + \mathbf{J}^{\text{ext}}(\mathbf{q}, \omega) \tag{4}$$

in the framework of linear response theory. In compact form, the wave equation hence can be written as

$$\mathbf{L}(\mathbf{q},\omega)\cdot\mathbf{E}(\mathbf{q},\omega) = -i\mu_0\omega\mathbf{J}^{\mathrm{ext}}(\mathbf{q},\omega), \tag{5}$$

where

$$\mathbf{L}(\mathbf{q},\omega) = \left[\left(\frac{\omega}{c}\right)^2 - q^2\right]\mathbf{U} + \mathbf{q}\mathbf{q} + i\mu_0\omega\boldsymbol{\sigma}(\mathbf{q},\omega). \tag{6}$$

By insertion of Eq. (2), the algebraic $\mathbf{L}(\mathbf{q},\omega)$ operator can be given the dyadic form

$$\mathbf{L}(\mathbf{q},\omega) = N_T(q,\omega)(\mathbf{U} - \hat{\mathbf{q}}\hat{\mathbf{q}}) + N_L(q,\omega)\hat{\mathbf{q}}\hat{\mathbf{q}}, \tag{7}$$

where

$$N_T(q,\omega) = \left(\frac{\omega}{c}\right)^2\left(1 + \frac{i}{\varepsilon_0\omega}\sigma_T(q,\omega)\right) - q^2, \tag{8}$$

$$N_L(q,\omega) = \left(\frac{\omega}{c}\right)^2\left(1 + \frac{i}{\varepsilon_0\omega}\sigma_L(q,\omega)\right). \tag{9}$$

The quantities

$$\varepsilon_T(q,\omega) = 1 + \frac{i}{\varepsilon_0\omega}\sigma_T(q,\omega), \tag{10}$$

$$\varepsilon_L(q,\omega) = 1 + \frac{i}{\varepsilon_0\omega}\sigma_L(q,\omega) \tag{11}$$

may be recognized as the microscopic transverse $[\varepsilon_T(q,\omega)]$ and longitudinal $[\varepsilon_L(q,\omega)]$ dielectric functions of the jellium.

Let us now introduce the algebraic dyadic propagator $\mathbf{G}(\mathbf{q},\omega)$ as the solution to

$$\mathbf{L}(\mathbf{q},\omega)\cdot\mathbf{G}(\mathbf{q},\omega) = \mathbf{U}. \tag{12}$$

On the basis of Eq. (7), it readily appears that $\mathbf{G}(\mathbf{q},\omega)$ is given by

$$\mathbf{G}(\mathbf{q},\omega) = \mathbf{L}^{-1}(\mathbf{q},\omega) = \frac{\mathbf{U} - \hat{\mathbf{q}}\hat{\mathbf{q}}}{N_T(q,\omega)} + \frac{\hat{\mathbf{q}}\hat{\mathbf{q}}}{N_L(q,\omega)}. \tag{13}$$

The derivation leading up to the result in Eq. (13) is not new [13], but the form of $\mathbf{G}(\mathbf{q},\omega)$ is of significant importance for what follows. The general solution to Eq. (5) thus can be written as

$$\mathbf{E}(\mathbf{q},\omega) = \mathbf{E}^{(0)}(\mathbf{q},\omega) - i\mu_0\omega\mathbf{G}(\mathbf{q},\omega)\cdot\mathbf{J}^{\mathrm{ext}}(\mathbf{q},\omega), \tag{14}$$

where $\mathbf{E}^{(0)}$ is a solution to the homogeneous ($\mathbf{J}^{\mathrm{ext}} = \mathbf{0}$) part of the wave equation.

C. Weyl expansion of the screened propagator

Although it is obvious from Eq. (13) that the wave equation (14) can be divided into two parts which describe, respectively, the transverse $\mathbf{E}_T = (\mathbf{U} - \hat{\mathbf{q}}\hat{\mathbf{q}})\cdot\mathbf{E}$ and longitudinal $\mathbf{E}_L = \hat{\mathbf{q}}\hat{\mathbf{q}}\cdot\mathbf{E}$ electrodynamics with respect to a given $\hat{\mathbf{q}}$ direction, this decomposition is not so useful for the present theory. Generally speaking, this is so because in every experimental situation the excitation of the jellium must require a finite-size jellium (metal, free-electron-like semiconductor, etc.). Being interested in surface excitations of a jellium with spatial (nonlocal) response, for a simple plane surface, the Weyl expression is particularly useful, as we will realize below.

The Weyl expansion of the propagator describes this in a mixed spatial domain: A 2D wave-vector and 1D direct-space combination. Thus, the Weyl expansion is

$$\mathbf{G}(\mathbf{q}_\parallel,\omega;Z) = \int_{-\infty}^{\infty}\mathbf{G}(\mathbf{q},\omega)e^{iq_\perp Z}\frac{dq_\perp}{2\pi}, \tag{15}$$

with

$$\mathbf{q} = \mathbf{q}_\parallel + q_\perp\hat{\mathbf{z}}, \tag{16}$$

Fourier transforming back to direct space in the (arbitrary) $\hat{\mathbf{z}}$ direction of a Cartesian coordinate system with unit vectors $(\hat{\mathbf{x}},\hat{\mathbf{y}},\hat{\mathbf{z}})$. Thus $\mathbf{q}_\parallel = q_{\parallel,x}\hat{\mathbf{x}} + q_{\parallel,y}\hat{\mathbf{y}}$. In cases where only one $\mathbf{q}_\parallel$ direction is involved it is convenient to take, e.g., $\mathbf{q}_\parallel = q_{\parallel,x}\hat{\mathbf{x}}$. In the Weyl expansion given in Eq. (15), one must write q as $q = (q_\parallel^2 + q_\perp^2)^{1/2}$ and $\hat{\mathbf{q}}$ as $\hat{\mathbf{q}} = (\mathbf{q}_\parallel + q_\perp\hat{\mathbf{z}})/(q_\parallel^2 + q_\perp^2)^{1/2}$ in the expression for $\mathbf{G}(\mathbf{q},\omega)$ [Eq. (13)]. Thus,

$$\mathbf{G}(\mathbf{q},\omega) = \frac{1}{q_\parallel^2 + q_\perp^2}\left(\frac{(q_\parallel^2 + q_\perp^2)\mathbf{U} - (\mathbf{q}_\parallel + q_\perp\hat{\mathbf{z}})(\mathbf{q}_\parallel + q_\perp\hat{\mathbf{z}})}{N_T[(q_\parallel^2 + q_\perp^2)^{1/2},\omega]} + \frac{(\mathbf{q}_\parallel + q_\perp\hat{\mathbf{z}})(\mathbf{q}_\parallel + q_\perp\hat{\mathbf{z}})}{N_L[(q_\parallel^2 + q_\perp^2)^{1/2},\omega]}\right). \tag{17}$$

D. Collective excitations: Pole contributions to $\mathbf{G}(\mathbf{q}_\parallel\omega, Z)$

The integrand in Eq. (15) is singular for $q_\perp = \kappa_\perp^T$ and $q_\perp = \kappa_\perp^L$, where

$$N_T(q_\parallel,\kappa_\perp^T,\omega) = \left(\frac{\omega}{c}\right)^2\varepsilon_T(q_\parallel,\kappa_\perp^T,\omega) - q_\parallel^2 - (\kappa_\perp^T)^2 = 0, \tag{18}$$

$$N_L(q_\parallel,\kappa_\perp^L,\omega) = \left(\frac{\omega}{c}\right)^2\varepsilon_L(q_\parallel,\kappa_\perp^L,\omega) = 0. \tag{19}$$

Physically, the collective plasmariton (T) and plasmon (L) bulk dispersion relations are given in indirect form by Eqs. (18) and (19). Under the assumption that the poles in Eq. (17) are of first order, a residue calculation in a complex $q_\perp$ plane allows one to evaluate the integral in Eq. (15) [with Eq. (17) inserted]. In terms of the upper-half-plane (superscript +) residues

$$\mathcal{R}_{T,L}^{(+)}(q_\parallel,\omega) = \lim_{q_\perp\to\kappa_\perp^{T,L}}\left(\frac{q_\perp - \kappa_\perp^{T,L}}{N_{T,L}(q_\parallel,q_\perp,\omega)}\right) = \left(\left.\frac{\partial N_{T,L}(q_\parallel,q_\perp,\omega)}{\partial q_\perp}\right|_{q_\perp\to\kappa_\perp^{L,T}}\right)^{-1}, \tag{20}$$

one obtains the following result for the two parts of the screened propagator:

$$\mathbf{G}_T(\mathbf{q}_\parallel,\omega;Z) = i\mathcal{R}_T^{(+)}(q_\parallel,\omega)\big[(\mathbf{U} - \hat{\mathbf{Q}}_+^T\hat{\mathbf{Q}}_+^T)e^{i\kappa_\perp^T Z}\theta(Z) + (\mathbf{U} - \hat{\mathbf{Q}}_-^T\hat{\mathbf{Q}}_-^T)e^{-i\kappa_\perp^T Z}\theta(-Z)\big] \tag{21}$$

and

$$\mathbf{G}_L(\mathbf{q}_\parallel,\omega;Z) = i\mathcal{R}_L^{(+)}(q_\parallel,\omega)\big[\hat{\mathbf{Q}}_+^L\hat{\mathbf{Q}}_+^L e^{i\kappa_\perp^L Z}\theta(Z) + \hat{\mathbf{Q}}_-^L\hat{\mathbf{Q}}_-^L e^{-i\kappa_\perp^T Z}\theta(-Z)\big]. \tag{22}$$

The explicit expression for $\hat{\mathbf{Q}}_\pm^T$ and $\hat{\mathbf{Q}}_\pm^L$ are given in Eqs. (A5) and (A6) of Appendix A, where aspects of the residue calculation are described.

E. Fundamental integral equation for the electric field

It follows from Eq. (14) that the microscopic electric field in the Weyl expansion is determined by the integral equation

$$\mathbf{E}(\mathbf{q}_\parallel,\omega;z)=\mathbf{E}^{(0)}(\mathbf{q}_\parallel,\omega;z)-i\mu_0\omega\int_{-\infty}^{\infty}\times\mathbf{G}(\mathbf{q}_\parallel,\omega;z-z')\cdot\mathbf{J}^{\text{ext}}(\mathbf{q}_\parallel,\omega;z')dz',\quad(23)$$

with $\mathbf{G}(\mathbf{q}_\parallel,\omega;z-z')$ given in the collective-mode approximation by the sum of $\mathbf{G}_T(\mathbf{q}_\parallel,\omega;z-z')$ [Eq. (21)] and $\mathbf{G}_L(\mathbf{q}_\parallel,\omega;z-z')$ [Eq. (22)]. In the remaining part of this paper we will be interested in studying this integral equation in the particularly simple case where the external current density can be approximated by an expression with only δ-function support in the z direction, i.e.,

$$\mathbf{J}^{\text{ext}}(\mathbf{q}_\parallel,\omega;z)=\mathbf{J}_0^{\text{ext}}(\mathbf{q}_\parallel,\omega)\delta(z-z_0),\quad(24)$$

where the current density sheet is supposed to be located at $z=z_0$. Our main effort will be devoted to an analysis of the eigenmode structure of the field, obtained from Eq. (23) setting $\mathbf{E}^{(0)}(\mathbf{q}_\parallel,\omega;z)=\mathbf{0}$.

III. SPATIALLY ONE-DIMENSIONALLY CONFINED FIELDS IN THE WEYL EXPANSION

A. Jump conditions of the electromagnetic field across an external current sheet

As a primer to the introduction of what we call the bulk jellion concept, we first derive the jump conditions for the electromagnetic field across a current density sheet in our infinite medium. The boundary conditions at a flat interface between two media are well known even in the presence of a current density perpendicular to the interface [14], and recently the dispersion relation for surface plasmaritons at a surface with a spatially local dielectric function has been derived in the case with dynamic (active) boundary conditions [15]. The external current density sheet is placed in a jellium with a spatially nonlocal dynamics, described here via the Weyl expansion of the propagator; see Eqs. (15), (A1), and (21)–(23) and recall that only collective plasmariton and plasmon modes are included.

Let us consider the jump in the microscopic electric field across an external current density sheet carrying a current density confined to the $\hat{\mathbf{q}}_\parallel-\hat{\mathbf{z}}$ plane (where $\hat{\mathbf{q}}_\parallel=\mathbf{q}_\parallel/q_\parallel$). For definiteness, we locate the sheet in the plane $z=z_0$. For our infinitely extended medium it is clear that the final result cannot depend on z_0. Thus, the current density $\mathbf{J}_0^{\text{ext}}(q_\parallel,\omega)$ of Eq. (24) takes the form

$$\mathbf{J}_0^{\text{ext}}(\mathbf{q}_\parallel,\omega)=J_{0,\parallel}^{\text{ext}}(\mathbf{q}_\parallel,\omega)\hat{\mathbf{q}}_\parallel+J_{0,z}^{\text{ext}}(\mathbf{q}_\parallel,\omega)\hat{\mathbf{z}}.\quad(25)$$

For the jump in the electric field across the plane $z=z_0$ we use the notation

$$\|\mathbf{E}\|\equiv\mathbf{E}(z\to z_0^+)-\mathbf{E}(z\to z_0^-).\quad(26)$$

For brevity, we leave out the notation $(\mathbf{q}_\parallel,\omega)$ from the two fields on the right-hand side of Eq. (26) and in most of the quantities appearing below. The jump $\|\mathbf{E}(\mathbf{q}_\parallel,\omega)\|\equiv\|\mathbf{E}\|$ is independent of z_0. The reader may find some details of the explicit calculation of $\|\mathbf{E}\|$ in Appendix B. Here we present only the physically important final result. With the abbreviation

$$\mathcal{H}=2\mu_0\omega q_\parallel\left(\frac{\mathcal{R}_L^{(+)}\kappa_\perp^L}{\kappa_L^2}-\frac{\mathcal{R}_T^{(+)}\kappa_\perp^T}{\kappa_T^2}\right),\quad(27)$$

where

$$\kappa_{T,L}^2=q_\parallel^2+(\kappa_\perp^{T,L})^2,\quad(28)$$

one obtains

$$\|\mathbf{E}\|=\mathcal{H}\big(J_{0,z}^{\text{ext}}\hat{\mathbf{q}}_\parallel+J_{0,\parallel}^{\text{ext}}\hat{\mathbf{z}}\big),\quad(29)$$

a result independent of z_0. Notice that the term in the large parentheses is *not* the current density. Hence, a current density in the plane of the sheet gives rise only to a jump in the component of the electric field perpendicular to the sheet plane. Oppositely, a current density in the $\hat{\mathbf{z}}$ direction results in a field jump in the component along $\hat{\mathbf{q}}_\parallel$. We will put this result in perspective soon. The jump in the magnetic field, viz.,

$$\|\mathbf{B}\|\equiv\mathbf{B}(z\to z_0^+)-\mathbf{B}(z\to z_0^-),\quad(30)$$

is given by

$$\|\mathbf{B}\|=2\mu_0\mathcal{R}_T^{(+)}\kappa_\perp^T J_{0,\parallel}^{\text{ext}}\hat{\mathbf{z}}\times\hat{\mathbf{q}}_\parallel\quad(31)$$

(see Appendix B).

B. Jump condition in local electrodynamics

In order to make the bridge from the perhaps more-well-known jump conditions in the limit where spatial dispersion is neglected [15] to the results in Eqs. (29) and (31), we make use of the result

$$\mathcal{R}_T^{(+)}=-\frac{1}{2\kappa_\perp^T},\quad(32)$$

which holds also in nonlocal electrodynamics in the framework of the Lindhard formalism (see Appendix C in Ref. [16]). Furthermore, the L mode is neglected because this only exists in the framework of a nonlocal approach [cf., e.g., Eq. (19)].

With these two simplifications, one obtains the jump conditions

$$\|\mathbf{D}\|=\varepsilon_0\varepsilon(\omega)\|\mathbf{E}\|=\frac{q_\parallel}{\omega}\big(J_{0,z}^{\text{ext}}\hat{\mathbf{q}}_\parallel+J_{0,\parallel}^{\text{ext}}\hat{\mathbf{z}}\big),\quad(33)$$

$$\|\mathbf{B}\|=-\mu_0J_{0,\parallel}^{\text{ext}}\hat{\mathbf{z}}\times\hat{\mathbf{q}}_\parallel.\quad(34)$$

These formulas are in complete agreement with the result obtained from an active vacuum-jellium interface [viz., $\varepsilon_0\|E_\parallel\|=(q_\parallel/\omega)J_{0,z}^{\text{ext}}$, $\|D_z\|=(q_\parallel/\omega)J_{0,\parallel}^{\text{ext}}$, and $\|B_{\hat{\mathbf{z}}\times\hat{\mathbf{q}}_\parallel}\|=-\mu_0J_{0,\parallel}^{\text{ext}}$] by replacing the vacuum with a medium with a dielectric constant $\varepsilon_0\varepsilon(\omega)$ (see Ref. [15]). This replacement only affects the jump condition for $\|E_\parallel\|$, i.e., $\varepsilon_0\|E_\parallel\|\Rightarrow\varepsilon_0\varepsilon(\omega)\|E_\parallel\|$, as the reader my verify by consulting, for instance, Ref. [14]. We will see this connection to Eqs. (33) and (34) in a direct fashion when we use the Weyl expansion of a propagator relating to a semi-infinite vacuum-jellium interface in Sec. V C.

C. Jellions: Entangled plasmon and plasmariton modes

The collective-mode structure of the screened propagator appears in a physically transparent manner if one introduces the generally complex four unit vectors

$$\mathbf{e}_{\pm}^{T} = \frac{1}{\kappa_T}(\pm\kappa_{\perp}^{T}\hat{\mathbf{x}} - q_{\parallel}\hat{\mathbf{z}}), \tag{35}$$

$$\mathbf{e}_{\pm}^{L} = \frac{1}{\kappa_L}(q_{\parallel}\hat{\mathbf{x}} \pm \kappa_{\perp}^{L}\hat{\mathbf{z}}), \tag{36}$$

where $\kappa_{T,L} = [q_{\parallel}^2 + (\kappa_{\perp}^{T,L})^2]^{1/2}$. The vectors in Eq. (35) and (36) relate to the choice $\mathbf{q}_{\parallel} = q_{\parallel}\hat{\mathbf{x}}$, which is convenient for what follows. These vectors are polarization unit vectors for the plasmariton (T) and plasmon (L) modes in the two half spaces $z > z_0$ (+ sign) and $z < z_0$ (− sign).

The tensorial structure of the propagators $\mathbf{G}_T(\mathbf{q}_{\parallel}, \omega; Z)$ and $\mathbf{G}_L(\mathbf{q}_{\parallel}, \omega; Z)$ can be expressed in terms of the polarization unit vectors. Thus

$$\mathbf{U} - \hat{\mathbf{Q}}_{\pm}^{T}\hat{\mathbf{Q}}_{\pm}^{T} = \hat{\mathbf{y}}\hat{\mathbf{y}} + \mathbf{e}_{\pm}^{T}\mathbf{e}_{\pm}^{T}, \tag{37}$$

$$\hat{\mathbf{Q}}_{\pm}^{L}\hat{\mathbf{Q}}_{\pm}^{L} = \mathbf{e}_{\pm}^{L}\mathbf{e}_{\pm}^{L}, \tag{38}$$

as the reader may show. In fact, only the relation in Eq. (37) needs to be worked out since $\hat{\mathbf{Q}}_{\pm}^{L}$ [Eq. (A6)] are just the unit vectors $\mathbf{e}_{\pm}^{L}$ [Eq. (36)]. The $\hat{\mathbf{y}}\hat{\mathbf{y}}$ part of Eq. (37) is associated with s-polarized fields, which have no plasmon part, and these fields are of no interest here, so let us leave out the $\hat{\mathbf{y}}\hat{\mathbf{y}}$-propagator part below.

The p-polarized structure of the electric field outside the current density plane at $z = z_0$ is obtained from Eq. (B1). With

$$\mathbf{G}_T(z - z_0) = i\mathcal{R}_T^{(+)}\big[\mathbf{e}_{+}^{T}\mathbf{e}_{+}^{T}e^{i\kappa_{\perp}^{T}(z-z_0)}\Theta(z - z_0) + \mathbf{e}_{-}^{T}\mathbf{e}_{-}^{T}e^{-i\kappa_{\perp}^{T}(z-z_0)}\Theta(z_0 - z)\big], \tag{39}$$

$$\mathbf{G}_L(z - z_0) = i\mathcal{R}_L^{(+)}\big[\mathbf{e}_{+}^{L}\mathbf{e}_{+}^{L}e^{i\kappa_{\perp}^{L}(z-z_0)}\Theta(z - z_0) + \mathbf{e}_{-}^{L}\mathbf{e}_{-}^{L}e^{-i\kappa_{\perp}^{L}(z-z_0)}\Theta(z_0 - z)\big], \tag{40}$$

where $\mathrm{Im}\kappa_{\perp}^{T,L} \geqslant 0$, one obtains the result

$$\mathbf{E}(z) = \big[A_{+}^{T}\mathbf{e}_{+}^{T}e^{i\kappa_{\perp}^{T}(z-z_0)} + A_{+}^{L}\mathbf{e}_{+}^{L}e^{i\kappa_{\perp}^{L}(z-z_0)}\big]\Theta(z - z_0) + \big[A_{-}^{T}\mathbf{e}_{-}^{T}e^{-i\kappa_{\perp}^{T}(z-z_0)} + A_{-}^{L}\mathbf{e}_{-}^{L}e^{-i\kappa_{\perp}^{L}(z-z_0)}\big]\Theta(z_0 - z), \tag{41}$$

where

$$A_{\pm}^{T} = \mu_0\omega\mathcal{R}_T^{(+)}\big(\mathbf{e}_{\pm}^{T}\cdot\mathbf{J}_0^{\mathrm{ext}}\big), \tag{42}$$

$$A_{\pm}^{L} = \mu_0\omega\mathcal{R}_L^{(+)}\big(\mathbf{e}_{\pm}^{L}\cdot\mathbf{J}_0^{\mathrm{ext}}\big). \tag{43}$$

The plasmariton and plasmon modes appearing in the expression for the electric field $\mathbf{E}(z) \equiv \mathbf{E}(\mathbf{q}_{\parallel}, \omega; z)$ in the Weyl expansion are entangled. This means that one cannot excite a $(\mathbf{q}_{\parallel}, \omega)$ Weyl mode which has pure plasmariton or plasmon character. The entanglement follows from the fact that the complex unit vectors for the T and L modes are not orthogonal, i.e.,

$$\mathbf{e}_{\pm}^{T}\cdot\mathbf{e}_{\pm}^{L} \neq 0. \tag{44}$$

In consequence, one cannot make a choice for the sheet current density which results in either pure plasmariton or plasmon excitation. In Ref. [17] the name jellions was given to these new modes and the related quanta. We will use this name in the remaining part of our paper. As we will realize in Sec. V, these modes also appear in the form of surface jellions, which we claim are the fundamental modes in flat-surface excitation of a jellium.

IV. BULK JELLION EIGENMODES

It appears from Eqs. (41)–(43) that the degree of the plasmon-plasmariton entanglement depends on the external current density $\mathbf{J}_0^{\mathrm{ext}}$. In general, it cannot be justified to consider $\mathbf{J}_0^{\mathrm{ext}}$ as a prescribed quantity due to important screening effects from the jellium electrons.

In the framework of linear and spatially nonlocal electrodynamics, the current density $\mathbf{J}^{\mathrm{ext}}(\mathbf{q}_{\parallel}, \omega; z) \equiv \mathbf{J}^{\mathrm{ext}}(z)$ appearing in Eq. (33) is related to the microscopic electric field $\mathbf{E}(\mathbf{q}_{\parallel}, \omega; z) \equiv \mathbf{E}(z)$ by a constitutive relation of the form

$$\mathbf{J}^{\mathrm{ext}}(z) = \int_{\mathrm{ext}} \mathbf{S}(z, z')\cdot\mathbf{E}(z')dz', \tag{45}$$

where $\mathbf{S}(\mathbf{q}_{\parallel}, \omega; z, z') \equiv \mathbf{S}(z, z')$ is the response tensor. The jellion field, obtained by setting $\mathbf{E}^{(0)}(\mathbf{q}_{\parallel}, \omega; z) \equiv \mathbf{E}^{(0)}(z) = \mathbf{0}$ for all z in the range of $\mathbf{J}^{\mathrm{ext}}(z)$ [indicated by the subscript ext on the integral in Eq. (45)], hence satisfies the homogenous integral equation

$$\mathbf{E}(z) = \int_{\mathrm{ext}} \mathbf{K}(z, z')\cdot\mathbf{E}(z')dz', \tag{46}$$

with a dyadic kernel given by

$$\mathbf{K}(z, z') = -i\mu_0\omega\int_{\mathrm{ext}} \mathbf{G}(z - z'')\cdot\mathbf{S}(z'', z')dz''. \tag{47}$$

A rigorous determination of $\mathbf{S}(z, z')$ must be based on the field-dependent (many-body) Schrödinger equation, and only by invoking substantial simplifications in the analysis can an explicit expression for $\mathbf{S}(z, z')$ be given [18–24].

Self-sustaining jellion modes may be obtained from Eq. (46) by neglect of irreversible losses in $\mathbf{G}$ and $\mathbf{S}$. Although losses usually cannot be neglected from an experimental point of view, determination of these self-sustaining partially localized 1D modes is of great theoretical importance. Let us assume that the microscopic electric field across the ext domain has been calculated; then the current density entering Eqs. (42) and (43), viz.,

$$\mathbf{J}_0^{\mathrm{ext}} = \int_{\mathrm{ext}} \mathbf{J}^{\mathrm{ext}}(z)dz = \int_{\mathrm{ext}} \mathbf{S}(z, z')\cdot\mathbf{E}(z')dz'dz, \tag{48}$$

is known and the jellion field [Eq. (41)] can be determined.

V. SURFACE JELLIONS: DISPERSION RELATION

The perhaps most important application of the jellion concept appears in the form of surface jellion eigenmodes spatially confined (in one dimension) at a flat interface separating a spatially nonlocal jellium from vacuum. The surface jellions are the eigenmodes obtained, e.g., by the reflection of p-polarized light from the surface [16] and when a charged particle penetrates the jellium from vacuum. It has often been claimed that the interface eigenmodes are surface plasmons and surface plasmaritons. In general, this claim is incorrect, as we will realize.

A. Jellion field in the framework of the semiclassical infinite-barrier model

Let us assume that an electronically sharp interface located at the plane $z = 0$ separates vacuum ($z < 0$) and a homogeneous jellium ($z > 0$). Such an interface model is an idealization because it neglects the jellium selvedge (see Appendix D). In the well-known semiclassical infinite-barrier (SCIB) model [6,9,13], which (in an one-electron approximation) neglects the quantum interference between the incoming and reflected parts of the wave function of a jellium electron being scattered elastically of the surface, the boundary will be sharp. We will use the SCIB model in the following and realize that elements of the bulk jellion analysis can be transferred with little effort to the surface jellion description.

In the SCIB model the microscopic conductivity tensor relating to the Weyl expansion $\boldsymbol{\sigma}(\mathbf{q}_\parallel, \omega; z, z') \equiv \boldsymbol{\sigma}(z, z')$ has an ij component given by

$$\sigma_{ij}(z, z') = \Theta(z)\Theta(z')\left[\sigma_{ij}^{\infty}(z - z') + \zeta_j \sigma_{ij}^{\infty}(z + z')\right], \quad (49)$$

where

$$\zeta_j = \begin{cases} 1, & j = x, y \\ -1, & j = z. \end{cases} \quad (50)$$

The quantities $\boldsymbol{\sigma}^{\infty}$ and Θ are the conductivity tensor of an infinite jellium and the Heaviside unit step function, respectively. In the SCIB model the semi-infinite jellium is simulated by an infinitely extended medium. Provided the extended electric field has the specular reflection symmetry

$$E_j(-z) = \zeta_j E_j(z), \quad (51)$$

the ith component of the induced current density then is given by

$$\begin{aligned} J_i(z) &= \int_0^{\infty} \left[\sigma_{ij}^{\infty}(z - z') + \zeta_j \sigma_{ij}^{\infty}(z + z')\right] E_j(z') dz' \\ &= \int_{-\infty}^{\infty} \sigma_{ij}^{\infty}(z - z') E_j(z') dz', \quad z > 0. \end{aligned} \quad (52)$$

As indicated, the result holds in the jellium half space ($z > 0$) and the conductivity tensor is that of an infinitely extended jellium. For what follows we the omit the superscript ∞ from the conductivity to comply with the notation of Sec. II.

It follows from the analysis of Sec. II that the electric field of the bulk jellium, given in Eq. (41), stems from the sheet current density in Eq. (24). This tells us that the electric field of a surface jellion in the half space $z > 0$, viz.,

$$\mathbf{E}(z) = -i\mu_0\omega \int_{-\infty}^{\infty} \mathbf{G}(z - z') \cdot \mathbf{J}^{\text{fic}}(z') dz', \quad (53)$$

can be obtained using a fictitious (fic) sheet current density

$$\mathbf{J}^{\text{fic}}(\mathbf{q}_\parallel, \omega; z') = \mathbf{g}(\mathbf{q}_\parallel, \omega)\delta(z'). \quad (54)$$

Due to the antisymmetry of the z component of the electric field $E_z(-z) = -E_z(z)$, the fictitious current density has no z component, so $\mathbf{g} = (g_x, g_y, 0)$. Furthermore, the surface jellion is p polarized, implying that $g_y = 0$. With

$$\mathbf{g}(q_\parallel, \omega) = \begin{pmatrix} g(q_\parallel, \omega) \\ 0 \\ 0 \end{pmatrix}, \quad (55)$$

we have come to the conclusion that the SCIB model leads to an electric field of the surface jellion in the jellium half space given as

$$\mathbf{E}(z) = \boldsymbol{\Xi}_+(z) \cdot \mathbf{g}, \quad z > 0, \quad (56)$$

where

$$\boldsymbol{\Xi}_+(z) = \mu_0\omega\left[\mathcal{R}_T^{(+)} \mathbf{e}_+^T \mathbf{e}_+^T e^{i\kappa_\perp^T z} + \mathcal{R}_L^{(+)} \mathbf{e}_+^L \mathbf{e}_+^L e^{i\kappa_\perp^L z}\right]. \quad (57)$$

Since

$$\mathbf{e}_+^T \cdot \mathbf{g} = \frac{\kappa_\perp^T}{\kappa_T} g, \quad \mathbf{e}_+^L \cdot \mathbf{g} = \frac{q_\parallel}{\kappa_L} g, \quad (58)$$

one gets the entangled field

$$\mathbf{E}(z) = \mu_0\omega\left(\mathcal{R}_T^{(+)} \frac{\kappa_\perp^T}{\kappa_T} \mathbf{e}_+^T e^{i\kappa_\perp^T z} + \mathcal{R}_L^{(+)} \frac{q_\parallel}{\kappa_L} \mathbf{e}_+^L e^{i\kappa_\perp^L z}\right) g, \quad z > 0. \quad (59)$$

The associated Weyl expanded magnetic field, obtained from

$$\mathbf{B}(z) = \frac{\hat{\mathbf{y}}}{i\omega}\left(\frac{\partial E_x(z)}{\partial z} - iq_\parallel E_z(z)\right), \quad (60)$$

then becomes

$$\mathbf{B}(z) = \mu_0 \hat{\mathbf{y}} \mathcal{R}_T^{(+)} \kappa_\perp^T e^{i\kappa_\perp^T z} g, \quad z > 0. \quad (61)$$

In the vacuum half space, the field of the surface jellion can likewise be generated by a fictitious surface current density

$$\mathbf{J}^{\text{fic}}(\mathbf{q}_\parallel, \omega, z') = \mathbf{g}_0(\mathbf{q}_\parallel, \omega)\delta(z'). \quad (62)$$

One cannot expect *a priori* that the amplitudes

$$\mathbf{g}_0(q_\parallel, \omega) = \begin{pmatrix} g_0(q_\parallel, \omega) \\ 0 \\ 0 \end{pmatrix} \quad (63)$$

and $\mathbf{g}$ [Eq. (55)] are identical. Since there is no plasmon mode in the vacuum, it follows from Eqs. (41) and (42) that the surface jellion has a vacuum field part given by

$$\mathbf{E}(z) = \boldsymbol{\Xi}_-^0(z) \cdot \mathbf{g}_0, \quad (64)$$

where

$$\boldsymbol{\Xi}_-^0(z) = \mu_0\omega \mathcal{R}_{T,0}^{(+)} \mathbf{e}_{0,-}^T \mathbf{e}_{0,-}^T e^{-iq_\perp^0 z}, \quad z < 0, \quad (65)$$

with a unit polarization vector in the vacuum

$$\mathbf{e}_{0,-}^T = \frac{c}{\omega}(-q_\perp^0 \hat{\mathbf{x}} - q_\parallel \hat{\mathbf{z}}). \quad (66)$$

From Eq. (20) one obtains the vacuum residue

$$\mathcal{R}_{T,0}^{(+)} = -\frac{1}{2q_\perp^0}. \quad (67)$$

By combining Eqs. (64)–(67) one finally has

$$\mathbf{E}(z) = \frac{\mu_0 c}{2} \mathbf{e}_{0,-}^T e^{-iq_\perp^0 z} g_0, \quad z < 0, \quad (68)$$

and via Eq. (60)

$$\mathbf{B}(z) = \frac{\mu_0}{2}\hat{\mathbf{y}}e^{-iq_\perp^0 z}g_0, \quad z < 0. \tag{69}$$

The microscopic electric and magnetic fields of the surface jellion thus are given by Eqs. (59), (61), (68), and (69) in the SCIB model. Although fictitious surface currents are used to determine the electromagnetic field of the surface jellion, no external surface current density in the form related to Eq. (23) [with Eq. (24) inserted] appears in the framework of the SCIB model. As discussed in our recent paper on surface plasmaritons [15], an external current density will be present if selvedge dynamics is included or a quantum-well film is deposited at the jellium-vacuum interface.

B. Surface jellions with passive boundary conditions

For what we have called a dynamically passive boundary ($\mathbf{J}^{\text{ext}} = \mathbf{0}$), the jump boundary conditions for the electromagnetic field, discussed in detail in Ref. [15], imply that the components of the electric and magnetic fields in the surface plane are continuous, that is, for p polarization (i) $E_x(z\to 0^-) = E_x(z\to 0^+)$ and (ii) $B_y(z\to 0^-) = B_y(z\to 0^+)$. Applying these conditions to the surface jellion case, one obtains, respectively,

$$\left[\mathcal{R}_T^{(+)}\left(\frac{\kappa_\perp^T}{\kappa_T}\right)^2 + \mathcal{R}_L^{(+)}\left(\frac{q_\parallel}{\kappa_L}\right)^2\right]g = -\frac{1}{2}\left(\frac{c}{\omega}\right)^2 q_\perp^0 g_0 \tag{70}$$

and

$$\mathcal{R}_T^{(+)}\kappa_\perp^T g = \frac{g_0}{2}. \tag{71}$$

By combining Eqs. (70) and (71), one immediately obtains the dispersion relation for surface jellions

$$\mathcal{R}_T^{(+)}\left(\frac{\kappa_\perp^T}{\kappa_T}\right)^2 + \mathcal{R}_L^{(+)}\left(\frac{q_\parallel}{\kappa_L}\right)^2 + \mathcal{R}_T^{(+)}\frac{q_\perp^0\kappa_\perp^T}{q_0^2} = 0, \tag{72}$$

with the abbreviation $\omega/c = q_0$ (vacuum wave number).

As shown in Appendix C, the residues appearing in Eq. (72) are given by

$$\mathcal{R}_T^{(+)} = -\frac{1}{2\kappa_\perp^T}, \tag{73}$$

$$\mathcal{R}_L^{(+)} = \frac{1}{2}\left(\frac{c}{\omega}\right)^2 \kappa_\perp^L\left[1-\varepsilon_L^{-1}(q_\parallel,\omega)\right], \tag{74}$$

where $\varepsilon_L(q_\parallel,\omega) \equiv \varepsilon_L(q_\parallel, q_\perp^L = 0, \omega)$. In passing, one should note that the result in Eq. (73), when inserted in the boundary condition for the parallel component of the magnetic field [Eq. (71)], gives

$$g = -g_0. \tag{75}$$

The amplitudes of the two fictitious surface currents appearing in the analysis hence have the same magnitude but opposite phases. If one also makes use of the dispersion relation for bulk plasmaritons, viz.,

$$\kappa_T = \frac{\omega}{c}\varepsilon_T^{1/2}(\kappa_T,\omega), \tag{76}$$

a combination of Eqs. (72)–(74) and (76) shows that the surface jellion dispersion $q_\parallel = q_\parallel(\omega)$ can be written in the implicit form

$$q_\perp^0\varepsilon_T(\kappa_T,\omega) + \kappa_\perp^T + \left(\frac{q_\parallel}{\kappa_L}\right)^2\kappa_\perp^L\varepsilon_T(\kappa_T,\omega)\left[\varepsilon_L^{-1}(q_\parallel,\omega) - 1\right] = 0. \tag{77}$$

In the local limit, where no plasmons exist and $\varepsilon_T(\kappa_T,\omega) \to \varepsilon(\omega)$, the surface jellion dispersion relation in the SCIB model reduces to the one for the plasmariton field with passive boundary conditions, viz.,

$$\kappa_\perp^T + q_\perp^0\varepsilon(\omega) = 0. \tag{78}$$

The dispersion relation in Eq. (77) also appears as a resonance condition for p-polarized light reflection from a vacuum-jellium interface [16]. In this context, it is of importance, for instance, for electrodynamic surface dressing studies of moving electrons, not just phenomena related to Cherenkov-Landau surface shock waves [25].

C. Surface jellions with active boundary conditions

For a number of problems it is necessary to go beyond the SCIB model. Among these problems a microscopic understanding of the electrodynamics in the selvedge region poses a particularly difficult challenge. To the extent that it is meaningful in a first approximation to treat the selvedge dynamics on the basis of a sheet model approach, one adds to the SCIB model an active surface current density, adequately placed just outside the jellium half space (at $z = 0^-$). In its own right it is also of interest to consider the electrodynamics in cases where a quantum-well film is deposited at the vacuum-jellium interface. In our recent article on surface plasmaritons [15], a detailed discussion of active surface electrodynamics was given, emphasizing classical as well as photon wave-mechanical and second-quantized aspects. The surface plasmariton approach is valid in cases where the jellium response is treated on the basis of local electrodynamics. Below we extend the classical surface plasmariton approach to surface jellions, still within the framework of the sheet model approach.

For p-polarized fields the jump conditions for the tangential components of the microscopic electric and magnetic field are given by [15]

$$\|E_x\| = \frac{1}{\varepsilon_0}\frac{q_\parallel}{\omega}J_z^S, \tag{79}$$

$$\|B_y\| = -\mu_0 J_x^S \tag{80}$$

for monochromatic fields with a wave vector $\mathbf{q}_\parallel = q_\parallel\hat{\mathbf{x}}$ along the interface. The jump in $F \equiv E_x$ or B_y across the $z = 0$ plane above is defined as [cf. Eqs. (26) and (30)]

$$\|F\| \equiv F(0^+) - F(0^-) \tag{81}$$

and the external surface current density is $\mathbf{J}^S \equiv \mathbf{J}^S(\mathbf{q}_\parallel,\omega; z = 0)$.

From Eqs. (59) and (68) one obtains, recalling Eqs. (35), (36), and (66),

$$E_x(z \to 0^+) = \mu_0\omega\left[\mathcal{R}_T^{(+)}\left(\frac{\kappa_\perp^T}{\kappa_T}\right)^2 + \mathcal{R}_L^{(+)}\left(\frac{q_\parallel}{\kappa_L}\right)^2\right]g, \quad (82)$$

$$E_x(z \to 0^-) = -\frac{\mu_0\omega}{2}\left(\frac{c}{\omega}\right)^2 q_\perp^0 g_0, \quad (83)$$

and hence the following jump condition for the tangential component of the electric field:

$$\left[\mathcal{R}_T^{(+)}\left(\frac{\kappa_\perp^T}{\kappa_T}\right)^2 + \mathcal{R}_L^{(+)}\left(\frac{q_\parallel}{\kappa_L}\right)^2\right]g + \frac{1}{2}\left(\frac{c}{\omega}\right)^2 q_\perp^0 g_0 = \left(\frac{c}{\omega}\right)^2 q_\parallel J_z^S. \quad (84)$$

Since $2\mathcal{R}_T^{(+)}\kappa_\perp^T = -1$ [Eq. (C6)] one obtains from Eqs. (61) and (69) the limiting values

$$B_y(z \to 0^+) = -\frac{\mu_0}{2}g, \quad B_y(z \to 0^-) = \frac{\mu_0}{2}g_0, \quad (85)$$

and hence the following jump in the tangential component of the magnetic field:

$$\tfrac{1}{2}(g + g_0) = J_x^S. \quad (86)$$

By means of Eqs. (84) and (86), the unknown quantities g and g_0 can be given in terms of (J_x^S, J_z^S). However, to obtain a dispersion relation for surface jellions, it is necessary to relate the surface current density to the prevailing electric field on the current density sheet. As discussed in some detail in Ref. [15], one obtains quite generally (in 2×2 matrix notation)

$$\begin{pmatrix} J_x^S \\ J_z^S \end{pmatrix} = \begin{pmatrix} S_{xx} & S_{xz} \\ S_{zx} & S_{zz} \end{pmatrix}\begin{pmatrix} E_x(z \to 0^-) \\ E_x(z \to 0^-) \end{pmatrix}, \quad (87)$$

where $\mathbf{S}$ is the surface response function calculated in the limit where the sheet acts as an electric dipole (ED) receiver and emitter. In this limit the response has been called an ED-ED response [26]. In our surface plasmariton paper [15] it was shown how $\mathbf{S}$ can be obtained for a quantum-well surface layer on the basis of quantum mechanics.

In the present study Eq. (87) takes the general form

$$\begin{pmatrix} J_x^S \\ J_z^S \end{pmatrix} = -\frac{\mu_0\omega}{2}\left(\frac{c}{\omega}\right)^2 g_0 \begin{pmatrix} S_{xx} & S_{xz} \\ S_{zx} & S_{zz} \end{pmatrix}\begin{pmatrix} q_\perp^0 \\ q_\parallel \end{pmatrix}. \quad (88)$$

By a combination of Eqs. (84), (86), and (88), g and g_0 can be eliminated and the following dispersion relation obtained for surface jellions with active boundary conditions:

$$q_\perp^0 + \frac{q_\parallel}{\varepsilon_0\omega}(q_\perp^0 S_{zx} + q_\parallel S_{zz}) - 2\left(\frac{\omega}{c}\right)^2\left[\mathcal{R}_T^{(+)}\left(\frac{\kappa_\perp^T}{\kappa_T}\right)^2 + \mathcal{R}_L^{(+)}\left(\frac{q_\parallel}{\kappa_L}\right)^2\right] \times \left(1 + \frac{1}{\varepsilon_0\omega}(q_\perp^0 S_{xx} + q_\parallel S_{xz})\right) = 0. \quad (89)$$

If wished, the explicit expressions for the T and L residues given in Eqs. (73) and (74) can be inserted in Eq. (89).

In the local limit, where $\mathcal{R}_L^{(+)} = 0$, Eq. (89) takes the simplified form

$$\kappa_\perp^T + \varepsilon(\omega)q_\perp^0 + \frac{q_\perp^0}{\varepsilon_0\omega}\left[\varepsilon(\omega)q_\parallel\left(S_{zx} + \frac{q_\parallel}{q_\perp^0}S_{zz}\right) + \kappa_\perp^T\left(S_{xx} + \frac{q_\parallel}{q_\perp^0}S_{xz}\right)\right] = 0, \quad (90)$$

as the reader may verify using the dispersion relation for bulk plasmaritons [Eq. (76) with $\varepsilon_T(\kappa_T, \omega) \to \varepsilon(\omega)$] and the general relation $2\kappa_\perp^T\mathcal{R}_T^{(+)} = -1$. The dispersion relation (90) is identical to the one obtained in Ref. [15] and analyzed analytically and numerically for a jellium quantum-well interface dominated by diamagnetic and paramagnetic responses, respectively.

D. Exponentially confined eigenmodes

The central concept for an understanding of the physical properties of a wide class of surface jellions is the dispersion relation given in an implicit form for passive and active boundary conditions by Eqs. (72) and (89), respectively. Notwithstanding the extreme difficulties one is facing in solving these equations in general, let us assume that an explicit solution

$$\omega = \omega(q_\parallel) \quad (91)$$

has been obtained for a given (microscopic) jellium model. Usually, one finds that the dispersion relation has several branches. If needed, these may be distinguished by adding a subscript b to the frequency [$\omega(q_\parallel) \Rightarrow \omega_b(q_\parallel)$, $b = 1, 2, \ldots$]. For the angular spectrum (simple Weyl) the expansion $q_\parallel$ is real, and due to obvious symmetry one can limit the considerations to positive-$q_\parallel$ values. Self-sustaining surface jellions are described by real values of ω.

In the presence of irreversible loss mechanisms, described in the simplest approach by a relaxation time (τ) model, ω becomes complex, i.e., $\omega = \omega_R + i\omega_I$ (with $\omega_I < 0$). The surface jellion dispersion relation also can cover monochromatic modes ($\omega = \omega_R$) decaying along the jellium-vacuum surface. For such modes $q_\parallel$ is complex ($q_\parallel = q_\parallel^R + iq_\parallel^I$).

In the eigenmode limit ($\tau \to \infty$), where both ω and $q_\parallel$ are real, each of the three wave numbers $q_\parallel^0$, $\kappa_\perp^T$, and $\kappa_\perp^L$, characterizing the field behavior perpendicular to the surface, are either real or purely imaginary. Among the various possibilities, what one may call a confined surface jellion eigenmode stands out. For this mode all three underlying modes decay exponentially with the distance from the surface. The confined eigenmodes thus belong to the part of the $\omega - q_\parallel$ domain for which

$$q_\perp^0 = i|q_\perp^0|, \quad \kappa_\perp^T = i|\kappa_\perp^T|, \quad \kappa_\perp^L = i|\kappa_\perp^L|. \quad (92)$$

This part we call the confinement region.

VI. SURFACE JELLIONS IN THE HYDRODYNAMIC APPROACH

A. Hydrodynamic model and confinement conditions

In the hydrodynamic approach to electrodynamics, the transverse and longitudinal dielectric functions are given by

$$\varepsilon_T(\omega) = 1 - \frac{\omega_p^2}{\omega(\omega + i/\tau)}, \tag{93}$$

$$\varepsilon_L(q, \omega) = 1 - \frac{\omega_p^2}{\omega(\omega + i/\tau) - Dq^2} \tag{94}$$

in the relaxation time approximation, with the quantities ω_p, D, and τ denoting the bulk angular plasma frequency, the particle (electron) diffusion coefficient, and the relaxation time, respectively. In the numerical calculations to follow below we take [3,5,8] $D \approx \frac{3}{5}v_F^2$, where v_F is the electron Fermi velocity. For an electron density n, $\omega_p = (ne^2/m\varepsilon_0)^{1/2}$, where m is the effective electron mass, and e^2 is the squared electron charge. In Eq. (93) we have neglected the generally small spatial dispersion, i.e., $\varepsilon_T(\kappa_T, \omega) \approx \varepsilon_T(\omega) \equiv \varepsilon(\omega)$ (see Ref. [13]).

Let us now consider the confinement conditions for a given branch of a surface jellion eigenmode (remembering $\tau \to \infty$). In the vacuum half space where $q_\parallel^2 + (q_\perp^0)^2 = [\omega(q_\parallel)/c]^2$, exponential confinement requires that

$$(cq_\parallel)^2 - \omega^2(q_\parallel) > 0, \quad z < 0, \tag{95}$$

giving

$$|q_\perp^0| = \frac{1}{c}[(cq_\parallel)^2 - \omega^2(q_\parallel)]^{1/2}. \tag{96}$$

For the plasmariton (T) mode, where

$$\kappa_T^2 = \left(\frac{\omega(q_\parallel)}{c}\right)^2 \varepsilon_T[\omega(q_\parallel)] = \frac{1}{c^2}\left[\omega^2(q_\parallel) - \omega_p^2\right], \tag{97}$$

it follows from Eq. (28) that confinement is obtained for

$$\omega_p^2 + (cq_\parallel)^2 - \omega^2(q_\parallel) > 0, \tag{98}$$

and hence

$$|\kappa_\perp^T| = \frac{1}{c}\left[\omega_p^2 + (cq_\parallel)^2 - \omega^2(q_\parallel)\right]^{1/2}. \tag{99}$$

Exponential confinement of both the vacuum and T modes thus requires that

$$\omega(q_\parallel) < cq_\parallel, \tag{100}$$

where $q_\parallel$ and $\omega(q_\parallel)$ both positive quantities. For the plasmon (L) mode, where $\varepsilon_L(q, \omega) = 0$ [Eq. (19)], Eq. (94) leads to

$$\kappa_L^2 = \frac{1}{D}\left[\omega^2(q_\parallel) - \omega_p^2\right]. \tag{101}$$

Inserting this result in Eq. (28), it appears that L-mode confinement requires that

$$\omega(q_\parallel) < \left(\omega_p^2 + Dq_\parallel^2\right)^{1/2}, \tag{102}$$

and thus

$$|\kappa_\perp^L| = \frac{1}{D^{1/2}}\left[\omega_p^2 + Dq_\parallel^2 - \omega^2(q_\parallel)\right]^{1/2}. \tag{103}$$

All three modes underlying a surface jellion eigenmode are exponentially confined provided the conditions (100) and (102) are satisfied.

B. Three-branch dispersion relation

The dispersion relation for surface jellions with passive boundary conditions is obtained by inserting the specifics of the hydrodynamic model into Eq. (77). Since

$$\varepsilon_L^{-1}(q_\parallel, \omega) - 1 = \frac{\omega_p^2}{D(\kappa_\perp^L)^2} \tag{104}$$

and

$$\frac{\varepsilon(\omega)\omega_p^2}{D\kappa_L^2} = \left(\frac{\omega_p}{\omega}\right)^2, \tag{105}$$

one obtains in an implicit form the following dispersion relation:

$$\kappa_\perp^L[\kappa_\perp^T + q_\perp^0\varepsilon(\omega)] + q_\parallel^2[1 - \varepsilon(\omega)] = 0. \tag{106}$$

In the local limit $\kappa_\perp^L \to \infty$ (recalling $D \to 0$) and to uphold Eq. (106), the surface plasmariton dispersion relation given in Eq. (78) must be satisfied. In the electrostatic limit $c \to \infty$, use of $\kappa_\perp^T \to iq_\parallel$, $q_\perp^0 \to iq_\parallel$, and some simple algebra leads to the Ritchie dispersion relation for surface plasmons [27], namely,

$$q_\parallel = \frac{1 + \varepsilon(\omega)}{2}\left(\frac{\omega(\omega + i/\tau)}{D}\right)^{1/2}. \tag{107}$$

In the lossless limit $q_\parallel = \omega[1 - (\omega_p^s/\omega)^2]/D^{1/2}$, the familiar result.

How many branches does the dispersion relation have? To answer this question it is useful to rewrite Eq. (106) in the following form:

$$\pm 2\left(\frac{D}{\omega(\omega + i/\tau)}\right)^{1/2} q_\parallel^3 - \left[\left(\frac{\omega}{c}\right)^2 \frac{D}{\omega(\omega + i/\tau)} + 1 + \varepsilon(\omega)\right] q_\parallel^2 + \left(\frac{\omega}{c}\right)^2 \varepsilon(\omega) = 0. \tag{108}$$

Although the calculation leading from Eq. (106) to Eq. (108) in a sense is straightforward, it is somewhat cumbersome.

For each of the signs in front of the $q_\parallel^3$ term, one has a third degree equation in $q_\parallel$. It appears that if $q_\parallel^{(+)}$ is a solution to Eq. (108) with the plus sign in front of the first term, then $q_\parallel^{(-)} = -q_\parallel^{(+)}$ will be a solution to the equation with the minus sign. The six solutions therefore can be divided into two sets belonging to $\mathrm{Im}q_\parallel > 0$ and $\mathrm{Im}q_\parallel < 0$, respectively. For $\mathrm{Im}q_\parallel > 0$ the waves decay in the positive-x direction and for $\mathrm{Im}q_\parallel < 0$ the decay is in the negative-x direction. Using Al as an example, we have made numerical calculations of the three solutions belonging to $\mathrm{Im}q_\parallel > 0$. Hence, for positive real frequencies ω we show in Figs. 1 and 2 the numerical results obtained for $\mathrm{Re}q_\parallel$ and $\mathrm{Im}q_\parallel$ as a function of ω normalized to ω_p.

Let us look at the three branches of the dispersion relation $\omega = \omega(\mathrm{Re}q_\parallel)$ (Fig. 1). Asymptotically, the three branches collapse into two in the limits $\omega/\omega_p \to 0$ and $\omega/\omega_p \to \infty$. In the high-frequency limit the two branches coincide with the local ($D^{1/2} \to 0$) surface plasmariton dispersion relation (thick-line branch) and the electrostatic ($c \to \infty$) surface plasmon dispersion relation (dashed-line branch), both here for finite τ of course. It follows readily from Eq. (108) that for $D^{1/2} \to 0$

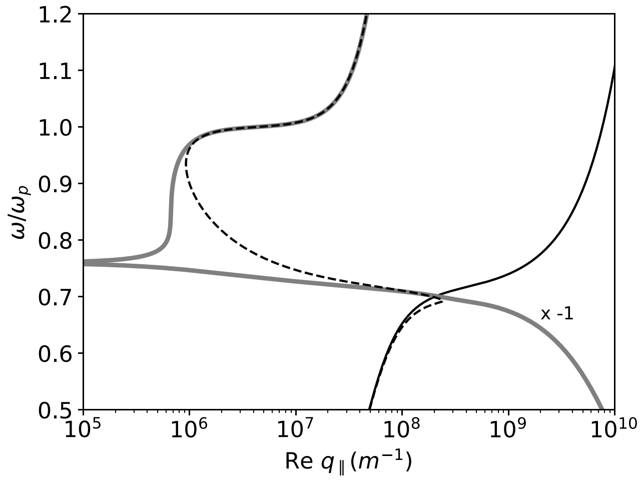

FIG. 1. Dispersion relation $\omega = \omega(\mathrm{Re}q_\parallel)$ (normalized to ω_p). The three branches are indicated by thick, thin, and dashed lines. Note that the thick-line branch has $\mathrm{Re}q_\parallel < 0$ for $\omega \lesssim \omega_p^s = \omega_p/\sqrt{2}$. The numerical calculations is for Al (jellium) electron density $n = 1.81\times10^{29}$ m^{-3}. The relaxation time used is $\tau = 7.5\times10^{-15}$ s. The values for n and τ are used in all subsequent calculations (figures) of this article. Qualitatively significant single-particle excitation effects (omitted in this paper) occur for $q_\parallel \gtrsim k_F \approx 1.8\times10^{10}$ m^{-1}.

one obtains the surface plasmariton dispersion relation in its standard form $q_\parallel = (\omega/c)\{\varepsilon(\omega)/[1+\varepsilon(\omega)]\}^{1/2}$. The radiative high-frequency branch of the local plasmariton dispersion relation commonly is called the Brewster branch [15]. At low frequencies, one recognizes the nonradiative Fano branch of the surface plasmariton dispersion relation (the coincident dashed and thin lines). For the thick-line branch the reader should notice that $\mathrm{Re}q_\parallel < 0$ for frequencies below a frequency close to the surface plasma frequency $\omega_p^s = \omega_p/\sqrt{2}$. In the lossless limit ($\tau \to \infty$) the crossover point is exactly at $\omega = \omega_p^s$. Below $\omega \approx \omega_p^s$ the phase velocity $\omega/\mathrm{Re}q_\parallel$ is negative. A negative phase velocity is not in itself an unphysical feature.

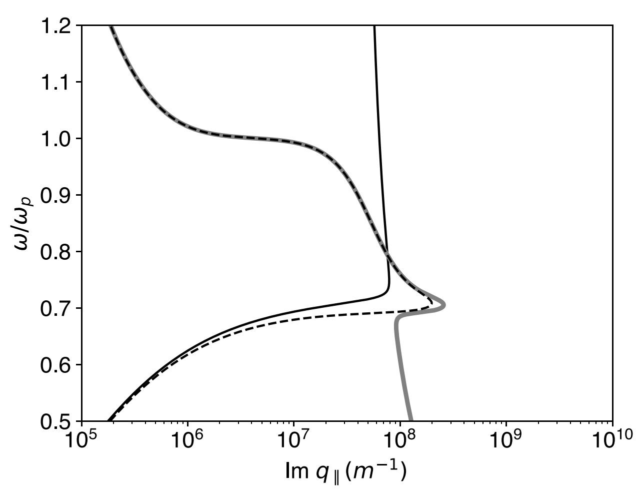

FIG. 2. Imaginary part of the wave number $\mathrm{Im}q_\parallel$ plotted as a function of ω (normalized to ω_p) for the three branches. As discussed in the text, branches with $\mathrm{Im}q_\parallel > 0$ are shown.

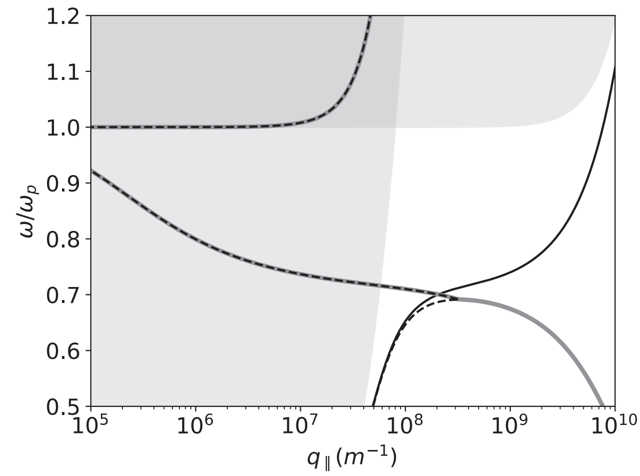

FIG. 3. Three-branch eigenmode dispersion relation $\omega = \omega(q_\parallel)$ (normalized to ω_p). The white domain in the $\omega/\omega_p - q_\parallel$ plane indicates the region in which the eigenmodes are exponentially confined [conditions (100) and (102) are both satisfied].

The presence of three distinct branches of the dispersion relation is a fingerprint of the plasmon-plasmariton entanglement. It appears from our numerical calculations (carried out now by letting τ increase towards infinity) that one for $\omega > 0$ still has six solutions for $q_\parallel$ which all have real $q_\parallel$ values. These can be divided into two sets belonging to $q_\parallel > 0$ and $q_\parallel < 0$. In each group the eigenmodes dispersion relation $\omega = \omega(q_\parallel)$ has three branches. The (inverse) dispersion relation in the two groups are related, as for finite τ, by $q_\parallel^{(-)} = -q_\parallel^{(+)}$. In Fig. 3 the branches of the eigenmodes are plotted for $q_\parallel > 0$, and the domain in the $\omega/\omega_p - q_\parallel$ plane in which the eigenmodes are exponentially confined is indicated as a white area.

The running eigenmodes for $q_\parallel > 0$ and $q_\parallel < 0$, belong to wave propagation in the positive- and negative-x direction, respectively. In Fig. 4 we have zoomed in on the $q_\parallel$ range in which the entanglement is most pronounced.

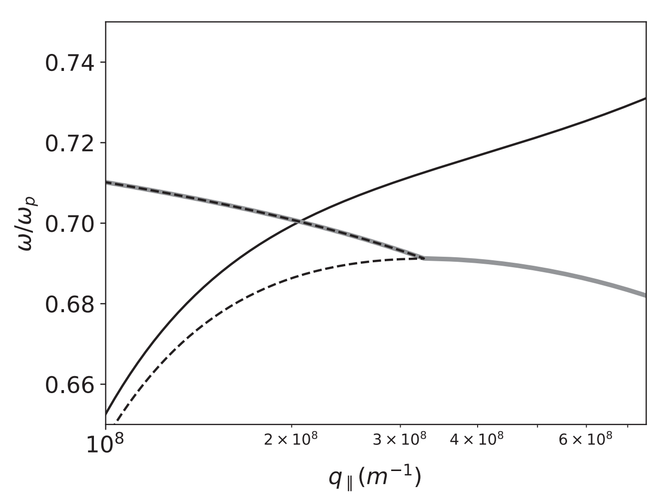

FIG. 4. Enlarged plot of the three branches of the eigenmode dispersion relation $\omega = \omega(q_\parallel)$ in the $q_\parallel$ range in which the surface plasmon-plasmariton entanglement is particularly pronounced.

In the framework of the hydrodynamic model, Moreau *et al.* [28] and Pitelet *et al.* [29] studied the effect of the surface density profile on the surface plasmariton dispersion relation. Their result was given in the form of a correction to Eq. (78), extended thus to $\kappa_\perp^T + q_\perp^0 \varepsilon(\omega) - i\varepsilon(\omega)\Omega = 0$, where $\Omega = \kappa_\perp^T/[(\kappa_\perp^T)^2 - \omega^2/D]$ in the collisionless limit. The results in [28,29] to some extent are a macroscopic counterpart to our surface active microscopic dispersion relation in Eq. (90). In a paper based on the Boltzmann transport equation and with a somewhat limited scope, a dispersion relation of the form given in Eq. (108) has been derived previously in relation to a study of the material and electromagnetic energy flow associated with surface electromagnetic waves [30].

VII. MOMENTA OF CONFINED SURFACE JELLION EIGENMODES

A. General result

In the framework of classical electrodynamics the total momentum of a global field plus particle system $\mathbf{P}_{\text{tot}}$ is the sum of the momenta of the particles $\mathbf{P}_{\text{par}} = \sum_\alpha \mathbf{p}_\alpha$ ($\mathbf{p}_\alpha$ is the momentum of particle α) and the electromagnetic field $\mathbf{P}_{\text{em}} \equiv \mathbf{P}$. The sum $\mathbf{P}_{\text{tot}} = \mathbf{P}_{\text{par}} + \mathbf{P}_{\text{em}}$ is a constant of the motion, that is, independent of time. In the following we focus our attention on the electromagnetic momentum of monochromatic surface jellions belonging to a given branch, described by the dispersion relation $\omega = \omega(q_\parallel)$. It is well known that (Re stands for the real part of)

$$\mathbf{P} = \varepsilon_0 \int_{-\infty}^{\infty} \mathbf{E}(\mathbf{r}, t) \times \mathbf{B}(\mathbf{r}, t) d^3 r$$
$$\approx \frac{\varepsilon_0}{2} \text{Re}\left(\int_{-\infty}^{\infty} \mathbf{E}(z; q_\parallel) \times \mathbf{B}^*(z; q_\parallel) d^3 r \right), \tag{109}$$

where the last expression holds if rapidly oscillating factors $\exp[\pm i 2\omega(q_\parallel)t]$ are, as usual, neglected. For an infinitely extended surface, the integration over the surface is carried out in the usual box ($L\times L$ area) normalization, i.e.,

$$\int_{-\infty}^{\infty} \int_{-\infty}^{\infty} dx\, dy \Rightarrow L^2. \tag{110}$$

Limiting ourselves to the field momenta of confined surface eigenmodes, the integral $\int_{-\infty}^{\infty} (\cdots) dz$ is finite. The plane-wave character of a given $q_\parallel$ mode ($\mathbf{q}_\parallel = q_\parallel \hat{\mathbf{x}}$) implies that the integrand in the second expression of Eq. (109), as indicated, is a function of z only [cf. Eq. (110)]. The field momentum

$$\mathbf{P} = \mathbf{P}_< + \mathbf{P}_> \tag{111}$$

is the sum of the momenta carried in vacuum ($\mathbf{P}_<$) and in the jellium ($\mathbf{P}_>$).

Let us first calculate $\mathbf{P}_<$. Recalling that $q_\perp^0 = i|q_\perp^0|$ [Eq. (92)] and $g_0 = -g$ [Eq. (75)], the electric and magnetic fields, obtained from Eqs. (68) and (69), are given by

$$\mathbf{E}(z; q_\parallel) = -\frac{\mu_0 c}{2} \mathbf{e}_{0,-}^T e^{|q_\perp^0| z} g, \tag{112}$$

with

$$\mathbf{e}_{0,-}^T = \frac{c}{\omega(q_\parallel)} (-i|q_\perp^0|\hat{\mathbf{x}} - q_\parallel \hat{\mathbf{z}}), \tag{113}$$

and

$$\mathbf{B}(z; q_\parallel) = -\frac{\mu_0}{2} \hat{\mathbf{y}} e^{|q_\perp^0| z} g. \tag{114}$$

Utilizing Eqs. (112)–(114), one obtains

$$\frac{\varepsilon_0}{2} \text{Re}[\mathbf{E}(z; q_\parallel) \times \mathbf{B}^*(z; q_\parallel)] = \frac{\mu_0 g g^*}{8\omega(q_\parallel)} \exp(2|q_\perp^0| z) q_\parallel \hat{\mathbf{x}}. \tag{115}$$

As expected, the momentum $\mathbf{P}_<$ is directed along $\mathbf{q}_\parallel = q_\parallel \hat{\mathbf{x}}$. Finally, integration over z (from $-\infty$ to 0) and box normalization give

$$\mathbf{P}_<(q_\parallel) = \frac{\mu_0 L^2 g g^*}{16} \frac{q_\parallel \hat{\mathbf{x}}}{\omega(q_\parallel)|q_\perp^0(q_\parallel)|}. \tag{116}$$

The determination of the momentum carried inside the jellium starts with the relevant expressions for $\mathbf{E}(z; q_\parallel)$ and $\mathbf{B}(z; q_\parallel)$, given in Eqs. (59) and (61). For the magnetic field one obtains immediately the expression

$$\mathbf{B}(z; q_\parallel) = -\frac{\mu_0}{2} \hat{\mathbf{y}} e^{-|\kappa_\perp^T| z} g. \tag{117}$$

In a sense this result may have been guessed: (i) The passive boundary condition for $\mathbf{B}$ gives $B_y(z \to 0^-; q_\parallel) = B_y(z \to 0^+; q_\parallel)$ and (ii) the $\mathbf{B}$ field decays exponentially in both half spaces. The electric field is, for confined surface jellions, given by ($\mathcal{R}_T^{(+)} \kappa_\perp^T = -\frac{1}{2}$)

$$\mathbf{E}(z; q_\parallel) = \mu_0 \omega \left(-\frac{1}{2\kappa_T^2} (i|\kappa_\perp^T|\hat{\mathbf{x}} - q_\parallel \hat{\mathbf{z}}) e^{-|\kappa_\perp^T| z} + \frac{q_\parallel \mathcal{R}_L^{(+)}}{\kappa_L^2} (q_\parallel \hat{\mathbf{x}} + i|\kappa_\perp^L|\hat{\mathbf{z}}) e^{-|\kappa_\perp^L| z} \right) g, \quad z > 0. \tag{118}$$

The expression for $\mathcal{R}_L^{(+)}$ [Eq. (74)] is a pure imaginary quantity for a confined L mode. Thus,

$$\mathcal{R}_L^{(+)} = iR|\kappa_\perp^L|, \tag{119}$$

where

$$R = \frac{1}{2} \left(\frac{c}{\omega(q_\parallel)} \right)^2 [1 - \varepsilon_L^{-1}(q_\parallel, \omega(q_\parallel))]. \tag{120}$$

Since only g may be complex in the expression for $\mathbf{B}(z; q_\parallel)$ [Eq. (117)] and $g^* g$ is real, only the real part of the factor to g in Eq. (118) contributes to Re$(\mathbf{E}\times\mathbf{B}^*)$. Therefore, since $-\hat{\mathbf{z}}\times\hat{\mathbf{y}} = \hat{\mathbf{x}}$, $\hat{\mathbf{z}}\times\hat{\mathbf{x}} = \hat{\mathbf{y}}$, and κ_T^2 and κ_L^2 are both real, one obtains

$$\frac{\varepsilon_0}{2} \text{Re}[\mathbf{E}(z; q_\parallel) \times \mathbf{B}^*(z; q_\parallel)]$$
$$= \frac{\mu_0 \omega(q_\parallel)}{4c^2} g g^* \left(\frac{1}{2\kappa_T^2} \exp(-2|\kappa_\perp^T| z) - \frac{R|\kappa_\perp^L|^2}{\kappa_L^2} \exp[-(|\kappa_\perp^T| + |\kappa_\perp^L|) z] \right) q_\parallel \hat{\mathbf{x}}, \quad z > 0. \tag{121}$$

Multiplying this momentum density by L^2 and integrating over z from 0 to ∞, we get our final result for the momentum in the jellium half space, viz.,

$$\mathbf{P}_>(q_\parallel) = \frac{\mu_0 L^2 g g^*}{16c^2}\omega(q_\parallel)\left(\frac{1}{\kappa_T^2|\kappa_\perp^T|} - \frac{4R}{\kappa_L^2}\frac{|\kappa_\perp^L|^2}{|\kappa_\perp^T| + |\kappa_\perp^L|}\right)q_\parallel \hat{\mathbf{x}},$$
$$z > 0. \tag{122}$$

B. Hydrodynamic model: Numerical results

The quantity R [Eq. (120)] is given by

$$R = \frac{1}{2}\left(\frac{c}{\omega(q_\parallel)}\right)^2 \frac{\omega_p^2}{\omega_p^2 + Dq_\parallel^2 - \omega^2} = \frac{1}{2}\left(\frac{c}{\omega(q_\parallel)}\right)^2 \frac{\omega_p^2}{D|\kappa_\perp^L|^2} \tag{123}$$

in the hydrodynamic model, with

$$D\kappa_L^2 = c^2\kappa_T^2 = \omega^2(q_\parallel) - \omega_p^2. \tag{124}$$

By inserting these results into Eq. (122) it appears that the field momentum in the jellium takes the hydrodynamic form

$$\mathbf{P}_>(q_\parallel) = \frac{\mu_0 L^2}{16}\frac{\omega(q_\parallel)}{\omega^2(q_\parallel) - \omega_p^2}\left[\frac{1}{|\kappa_\perp^T|} - 2\left(\frac{\omega_p}{\omega(q_\parallel)}\right)^2 \frac{1}{|\kappa_\perp^T| + |\kappa_\perp^L|}\right] g g^* q_\parallel \hat{\mathbf{x}}. \tag{125}$$

The essential $q_\parallel$ dependence in the vacuum and jellium half spaces are contained in the normalized (N) scalar quantities

$$P_{\gtrless}(q_\parallel) \equiv \frac{16}{\mu_0 L^2}\frac{1}{g g^*}\mathbf{P}_{\gtrless} \cdot \hat{\mathbf{x}}. \tag{126}$$

By multiplication by ω_p, one obtains the following dimensionless forms:

$$\omega_p P_<^N(q_\parallel) = \frac{\omega_p}{\omega(q_\parallel)}\left[1 - \left(\frac{\omega(q_\parallel)}{cq_\parallel}\right)^2\right]^{-1/2} \tag{127}$$

and

$$\omega_p P_>^N(q_\parallel) = \frac{\omega_p \omega(q_\parallel) q_\parallel}{\omega^2(q_\parallel) - \omega_p^2}\left[\frac{1}{|\kappa_\perp^T(q_\parallel)|} - 2\left(\frac{\omega_p}{\omega(q_\parallel)}\right)^2 \frac{1}{|\kappa_\perp^T| + |\kappa_\perp^L|}\right]. \tag{128}$$

The result of a numerical calculation of $\omega_p P_<^N(q_\parallel)$ and $\omega_p P_>^N(q_\parallel)$ for each of the three branches of the surface jellion eigenmodes is shown in Figs. 5 and 6, and the total quantity $\omega_p[P_<^N(q_\parallel) + P_>^N(q_\parallel)]$ is plotted in Fig. 7.

In the vacuum half space the field momentum is for all $q_\parallel$ directed in the $\mathbf{q}_\parallel$ direction, i.e., $\mathbf{P}_< \cdot \mathbf{q}_\parallel/q_\parallel > 0$. This result is obvious from Eq. (127) since $\omega(q_\parallel)/cq_\parallel < 1$ in the exponentially confined region.

C. Momentum backflow

It appears from Fig. 6 that the momenta inside the jellium in the major part of the $q_\parallel$ range shown are oppositely directed $\mathbf{q}_\parallel$, i.e., $\mathbf{P}_> \cdot \mathbf{q}_\parallel/q_\parallel < 0$. In a qualitative sense this backflow of the momenta originates in the sign of the factor $[\omega^2(q_\parallel) - \omega_p^2]^{-1}$ in Eq. (128). Thus, from the dispersion relations in the confinement region (Fig. 3), we see that $\omega(q_\parallel) < \omega_p$ except at the highest wave numbers for one of the branches. This branch is essentially the electrostatic plasmon branch since the L-T entanglement is vanishingly small at high wave numbers.

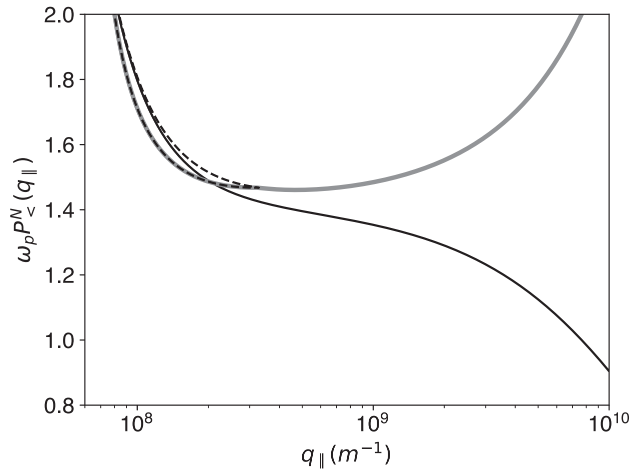

FIG. 5. Normalized (N) projection of the field momentum in vacuum in the $\hat{\mathbf{q}}_\parallel$ direction [$P_<^N(q_\parallel)$], made dimensionless [$\omega_p P_<^N(q_\parallel)$], as a function of the wave number $q_\parallel$. Plots are shown for each of the three confined surface jellion eigenmodes.

If we write Eq. (128) in the form

$$\omega_p \mathbf{P}_>^N(q_\parallel) = \frac{\omega_p \omega(q_\parallel) q_\parallel}{\omega^2(q_\parallel) - \omega_p^2}\frac{1}{|\kappa_\perp^T|}F(q_\parallel), \tag{129}$$

where

$$F(q_\parallel) = 1 - 2\left(\frac{\omega_p}{\omega(q_\parallel)}\right)^2\left[1 + \frac{|\kappa_\perp^L|}{|\kappa_\perp^T|}\right]^{-1}, \tag{130}$$

it appears that the main (qualitative) result of the momentum backflow is changed in the regions where $F(q_\parallel)$ becomes negative. Thus, where $F(q_\parallel) < 0$, the momentum flow is in the forward direction like in the vacuum domain. The

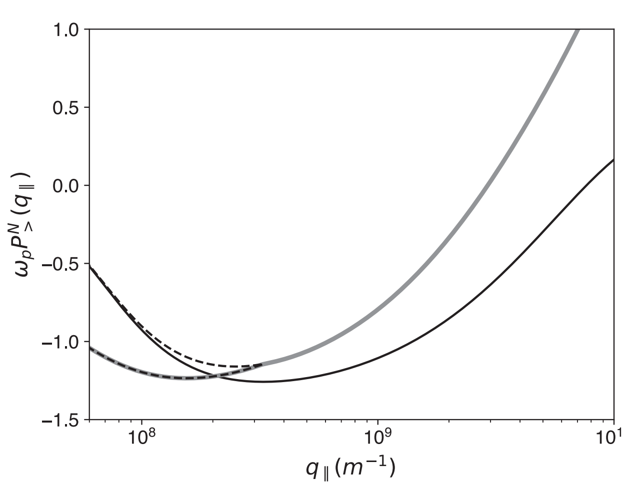

FIG. 6. Normalized (N) projection of the field momentum in jellium in the $\hat{\mathbf{q}}_\parallel$ direction [$P_>^N(q_\parallel)$], made dimensionless [$\omega_p P_>^N(q_\parallel)$], as a function of the wave number $q_\parallel$. Plots showing the momentum backflow are presented for each of the three confined surface jellion eigenmodes.

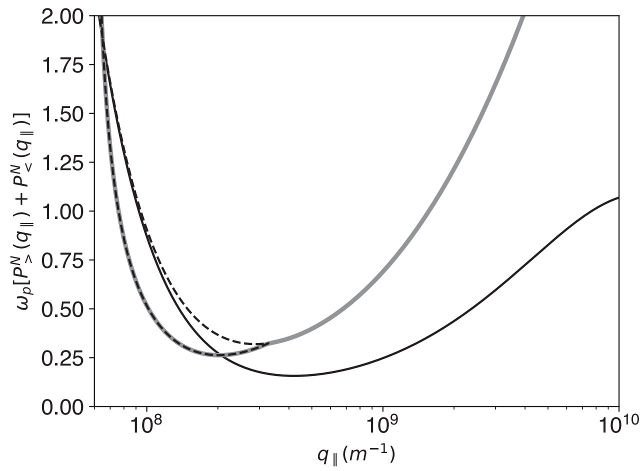

FIG. 7. Total dimensionless scalar momentum $\omega_p[P^N_<(q_\parallel)+P^N_>(q_\parallel)]$ for each of the three confined surface jellion eigenmodes plotted as a function of the wave number $q_\parallel$.

factor $[\omega_p/\omega(q_\parallel)]^2$ in front of the term in square brackets in Eq. (130) indicates that the change from backflow to forward flow happens first (with increasing $q_\parallel$) for the thick-line branch, as the reader may observe in comparing Figs. 3 and 6.

In closing this section one should note that the total momentum (in the various branches) of the global field plus particle system contains a part stemming from the kinetic momentum flow of the jellium electrons. This part, only nonvanishing in the presence of spatial dispersion, is always directed in the $\mathbf{q}_\parallel$ direction [30]. It is beyond the scope of this article to examine the momentum flow in the global system.

VIII. EQUIVALENT MASS OF CONFINED SURFACE JELLIONS

The Weyl representation of a given electromagnetic field is a mode representation, often called the angular spectrum representation [11]. This implies that the total energy of the jellion field is a sum of the energies of the individual $\mathbf{q}_\parallel$ modes.

A. Classical field Hamiltonian of a single Weyl mode

Below we focus on the field Hamiltonian $H(q_\parallel)$ belonging to a specific branch of the surface jellion with dispersion relation $\omega=\omega(q_\parallel)$. Furthermore, as in Sec. VII, we limit our study to the confined eigenmodes. It is for such modes that one can introduce an equivalent mass concept for the surface jellions, as we will realize in the following.

It is convenient for the general discussion to write the electric and the magnetic fields in the form

$$\mathbf{E}(z;q_\parallel)=\mathbf{V}_E(z;q_\parallel)g, \tag{131}$$

$$\mathbf{B}(z;q_\parallel)=\mathbf{V}_B(z;q_\parallel)g, \tag{132}$$

$$\mathbf{V}_E=[\boldsymbol{\Theta}_+(z;q_\parallel)\theta(z)-\boldsymbol{\Theta}^0_-(z;q_\parallel)\theta(-z)]\cdot\hat{\mathbf{x}}, \tag{133}$$

$$\mathbf{V}_B=-\frac{\mu_0}{2}\hat{\mathbf{y}}[e^{-|\kappa_\perp^T|z}\theta(z)+e^{|q_\perp^0|z}\theta(-z)]. \tag{134}$$

In the confinement regions

$$\boldsymbol{\Theta}_+(z;q_\parallel)\cdot\hat{\mathbf{x}}=\mu_0\omega\left(-\frac{1}{2\kappa_T^2}(i|\kappa_\perp^T|\hat{\mathbf{x}}-q_\parallel\hat{\mathbf{z}})e^{-|\kappa_\perp^T|z}\right.$$
$$\left.\times\frac{iR|\kappa_\perp^L|q_\parallel}{\kappa_L^2}(q_\parallel\hat{\mathbf{x}}+i|\kappa_\perp^L|\hat{\mathbf{z}})e^{-|\kappa_\perp^L|z}\right) \tag{135}$$

[see Eqs. (118) and (119)] and

$$-\boldsymbol{\Theta}^0_-\cdot\hat{\mathbf{x}}=-\frac{\mu_0c^2}{2}\frac{1}{\omega(q_\parallel)}(-i|q_\perp^0|\hat{\mathbf{x}}-q_\parallel\hat{\mathbf{z}}) \tag{136}$$

[from Eqs. (112) and (113)]. The total classical Hamiltonian (field energy) $H(q_\parallel)$ of a single mode hence is given by

$$H(q_\parallel)=\frac{\varepsilon_0}{4}gg^*\int_{-\infty}^{\infty}[|\mathbf{V}_E(z;q_\parallel)|^2+c^2|\mathbf{V}_B(z;q_\parallel)|^2]d^3r$$
$$=\frac{\varepsilon_0L^2}{4}gg^*\int_{-\infty}^{\infty}[|\mathbf{V}_E(z;q_\parallel)|^2+c^2|\mathbf{V}_B(z;q_\parallel|^2]dz, \tag{137}$$

where the last expression comes from the box $(L\times L)$ area normalization. In the exponential confinement region the integral $\int_{-\infty}^{\infty}(\cdots)dz$ is finite.

B. Surface jellion equivalent mass: Harmonic-oscillator description

In the confinement domain an equivalent mass concept can be introduced by the definition

$$M(q_\parallel)\equiv\int_{-\infty}^{\infty}[|\mathbf{V}_E(z;q_\parallel)|^2+c^2|\mathbf{V}_B(z;q_\parallel|^2]dz. \tag{138}$$

The reader should notice here that $M(q_\parallel)$ does not have the dimension of an usual mass. However, this fact is not of importance in what follows.

Let us now introduce a time-dependent quantity

$$g(t)=g\exp[-i\omega(q_\parallel)t] \tag{139}$$

and next a real coordinate variable by the definition

$$q(t)\equiv\frac{L}{2}\sqrt{\frac{\varepsilon_0}{2}}\frac{1}{\omega(q_\parallel)}[g(t)+g^*(t)], \tag{140}$$

with associated velocity

$$\dot{q}(t)=-i\frac{L}{2}\sqrt{\frac{\varepsilon_0}{2}}[g(t)-g^*(t)]. \tag{141}$$

Note that also the coordinate and velocity concepts do not have the usual dimension. Equations (140) and (141) can be inverted to give

$$g(t)=\frac{1}{L}\sqrt{\frac{2}{\varepsilon_0}}[\omega(q_\parallel)q(t)-i\dot{q}(t)]. \tag{142}$$

The product $g(t)g^*(t)$ is time independent and given by

$$g(t)g^*(t)=g(0)g^*(0)=\frac{2}{\varepsilon_0L^2}[\omega^2(q_\parallel)q^2(t)+\dot{q}^2(t)]. \tag{143}$$

By inserting Eq. (143) into Eq. (137) and with the equivalent mass concept it appears that the classical Hamiltonian can be written in the harmonic-oscillator form

$$H(q_\parallel) = \tfrac{1}{2}M(q_\parallel)[\omega^2(q_\parallel)q^2(t) + \dot{q}^2(t)]. \tag{144}$$

Introduction of a momentum variable

$$p(t) = M(q_\parallel)\dot{q}(t), \tag{145}$$

one obtains the form

$$H(q_\parallel) = \frac{p^2(t)}{2M(q_\parallel)} + \frac{M(q_\parallel)}{2}\omega^2(q_\parallel)q^2(t). \tag{146}$$

C. Quantization

The quantities $q(t)$ and $p(t)$ form a pair of real canonical variables, that is,

$$\dot{q} = \frac{\partial H}{\partial p}, \quad \dot{p} = -\frac{\partial H}{\partial q}, \tag{147}$$

where $\dot{q} = \frac{p}{M}$ and $\dot{p} = -M\omega^2(q_\parallel)q$, and the quantization now follows the textbook approach for a massive harmonic oscillator. The extension to the operator level, i.e., $q \Rightarrow \hat{q}$, $p \Rightarrow \hat{p}$, and $H \Rightarrow \hat{H}$, and introduction of the normalized (N) observables

$$\hat{q}_N \equiv \sqrt{\frac{M(q_\parallel)\omega(q_\parallel)}{\hbar}}\hat{q}, \quad \hat{p}_N \equiv \frac{1}{\sqrt{M(q_\parallel)\hbar\omega(q_\parallel)}}\hat{p}, \tag{148}$$

give

$$\hat{H} = \tfrac{1}{2}\hbar\omega(q_\parallel)\left[\hat{q}_N^2 + \hat{p}_N^2\right], \tag{149}$$

with the canonical commutation relation $[\hat{q}_N, \hat{p}_N] = i$ (obtained from $[\hat{q}, \hat{p}] = i\hbar$). By means of the annihilation and creation operators

$$\hat{a} = \frac{1}{\sqrt{2}}(\hat{q}_N + i\hat{p}_N), \quad \hat{a}^\dagger = \frac{1}{\sqrt{2}}(\hat{q}_N - i\hat{p}_N), \tag{150}$$

satisfying $[\hat{a}, \hat{a}^\dagger] = 1$, one obtains the standard form

$$\hat{H} = \hbar\omega(q_\parallel)\left[\hat{a}^\dagger\hat{a} + \tfrac{1}{2}\right], \tag{151}$$

giving the surface jellion quantum energy $\hbar\omega(q_\parallel)$ for the eigenmode with index $q_\parallel$.

D. Analysis of M: Numerical results for the hydrodynamic model

The close relation between the Hamiltonian H and the equivalent mass M [Eq. (137)] makes it of interest to study the structure of $M(q_\parallel)$ for each of the three branches of the eigenmode dispersion relation. The physical information carried by H and M essentially is the same since the two quantities [apart from the trivial constant $(\varepsilon_0/4)L^2$] only deviate by the absolute square of the SCIB model's fictitious sheet current density gg^*. The magnitude of gg^* is of course arbitrary for an eigenmode. In a p-polarized optical reflection experiment, with a known value of the incoming field energy, a specific value for gg^* follows.

Our quantitative analysis or interpretation of the M structure as a function of $q_\parallel$ partly is illustrated below by numerical results for the hydrodynamic model (using the Al data). In Fig. 8 the total equivalent mass $M = M_< + M_>$ is shown as a function of $q_\parallel$ for each of the three branches. In order to understand the underlying structure we have plotted $M_<$ and $M_>$ separately in Figs. 9 and 10.

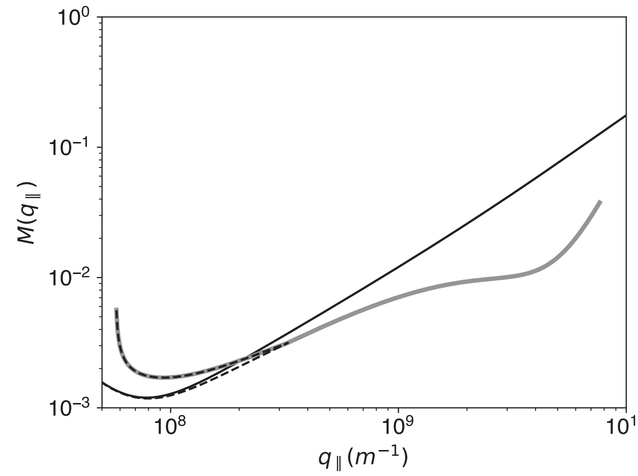

FIG. 8. Equivalent mass $M(q_\parallel)$ of each of the three confined surface jellion eigenmodes, given in arbitrary units, plotted as a function of the wave number $q_\parallel$.

Let us first consider the equivalent mass carried on the vacuum side of the surface. Since the electric and magnetic energy densities are equal in vacuum, one readily obtains

$$M_<(q_\parallel) = 2c^2\int_{-\infty}^{\infty}|\mathbf{V}_B(z;q_\parallel)|^2dz = \left(\frac{\mu_0 c}{2}\right)^2\frac{1}{|q_\perp^0|} \tag{152}$$

using Eq. (134). Since $q_\perp^0 = \{q_\parallel^2 - [\omega(q_\parallel)/c]^2\}^{1/2}$, $M_<$ essentially tends towards the same value for all branches at large-$q_\parallel$ values, viz.,

$$M_<(q_\parallel) = \left(\frac{\mu_0 c}{2}\right)^2\frac{1}{q_\parallel}, \quad q_\parallel \to \infty, \tag{153}$$

as Fig. 9 shows. The result is obvious for the two branches which have $\omega(q_\parallel) \lesssim 0.75\omega_p$ for all $q_\parallel$. For the Ritchie branch [Eq. (107), with $\tau \to \infty$] $\omega(q_\parallel) = D^{1/2}q_\parallel$ at large $q_\parallel$,

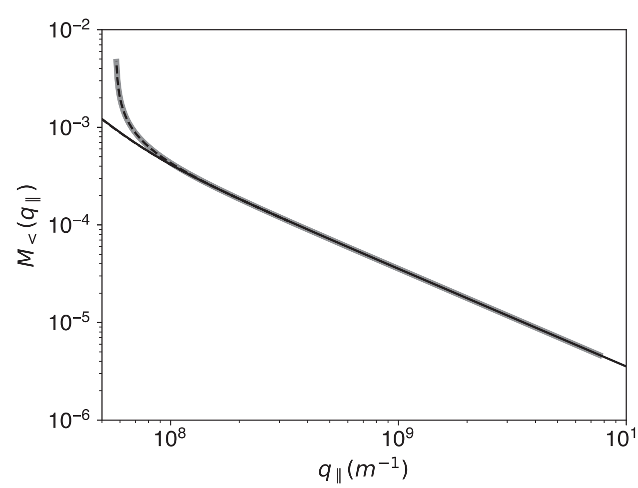

FIG. 9. Vacuum part of the equivalent mass $M_<(q_\parallel)$ of each of the three confined surface jellion eigenmodes, given in arbitrary units, plotted as a function of the wave number $q_\parallel$.

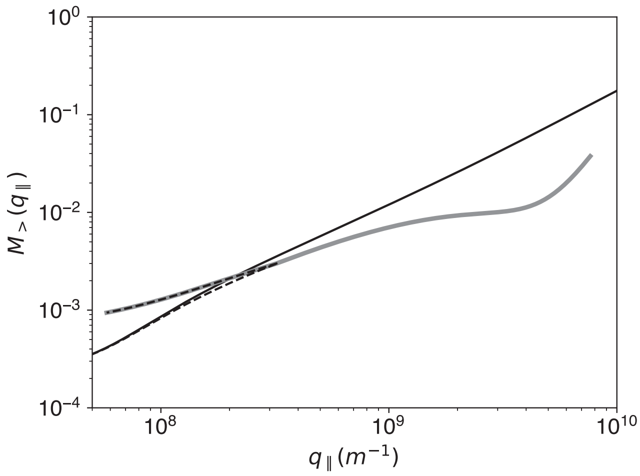

FIG. 10. Jellium part of the equivalent $M_>(q_\parallel)$ of each of the three confined surface jellion eigenmodes, given in arbitrary units, plotted as a function of the wave number $q_\parallel$. Note that the equivalent mass is scaled in the same manner in Figs. 8–10.

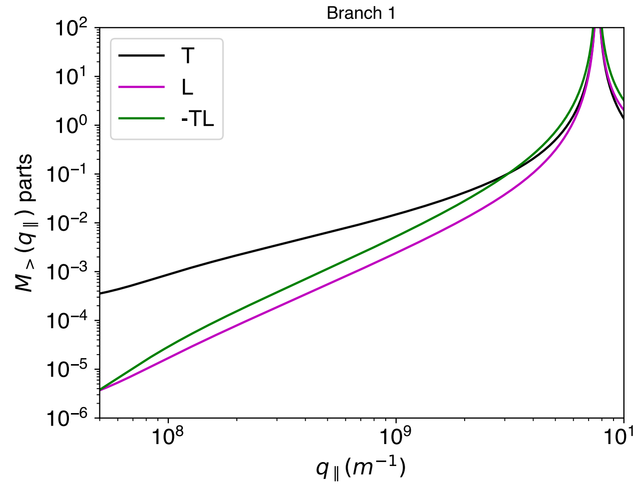

FIG. 11. Branch 1 (thin line in Fig. 3): Individual jellium equivalent mass contributions $M_>^T(q_\parallel)$, $M_>^L(q_\parallel)$, and $M_>^{TL}(q_\parallel)$ as functions of the wave number $q_\parallel$. Note that $M_>^{TL}(q_\parallel)$ is negative.

implying that $q_\perp^0 \to q_\parallel(1-D/c^2)^{1/2}$, thus giving an insignificant deviation of the order $D/c^2 \approx 10^{-4}$ from the asymptotic result in Eq. (153). The balance between the vacuum and jellium mass parts changes with increasing $q_\parallel$: $M_<(q_\parallel)$ decreases (as given by $q_\parallel^{-1}$) and $M_>(q_\parallel)$ increases for the three branches, as shown in Fig. 10.

The general expression for the mass carried in the jellium ($z>0$) can be calculated using Eqs. (133)–(135). It appears from Eq. (135) that the density $\mathbf{V}_E(z;\mathbf{q}_\parallel)\cdot\mathbf{V}_E^*(z;\mathbf{q}_\parallel)$ consists of three parts with the z dependences $\exp(-2|\kappa_\perp^T|z)$, $\exp(-2|\kappa_\perp^L|z)$, and $\exp[-(|\kappa_\perp^T|+|\kappa_\perp^L|)z]$. The magnetic mass contribution has the z dependence $\exp(-2|\kappa_\perp^T|z)$. The contributions of the T, L, and TL parts to the jellium mass are denoted by $M_>^T$, $M_>^L$, and $M_>^{TL}$, respectively. Note that $M_>^T$ is the sum of electric- and magnetic-field parts. The parts are additive, so

$$M_>(q_\parallel) = M_>^T(q_\parallel) + M_>^L(q_\parallel) + M_>^{TL}(q_\parallel). \tag{154}$$

Although a bit tedious, the calculation of the three parts to $M_>(q_\parallel)$ is straightforward and, as the reader may find on their own, the results are

$$M_>^T(q_\parallel) = \left(\frac{\mu_0\omega(q_\parallel)}{2\kappa_T^2}\right)^2 \frac{q_\parallel^2+|\kappa_\perp^T|^2}{2|\kappa_\perp^T|} + \left(\frac{\mu_0 c}{2}\right)^2 \frac{1}{2|\kappa_\perp^T|}, \tag{155}$$

where the last part is the **B**-field contribution. Note that this part can be obtained from the magnetic vacuum part $M_<(q_\parallel)/2$ by the replacement $|q_\perp^0| \to |\kappa_\perp^T|$. The sum $M_<(q_\parallel)+M_>^T(q_\parallel)$ is a pure surface plasmariton equivalent mass. The pure plasmon contribution to the equivalent mass is

$$M_>^L(q_\parallel) = \left(\frac{\mu_0\omega(q_\parallel)q_\parallel}{\kappa_L^2}\right)^2 (R|\kappa_\perp^L|)^2 \frac{q_\parallel^2+|\kappa_\perp^L|^2}{2|\kappa_\perp^L|}, \tag{156}$$

with R given by Eq. (120). The plasmon-plasmariton part of the equivalent mass is given by

$$M_>^{TL}(q_\parallel) = -\left(\frac{\mu_0\omega(q_\parallel)q_\parallel}{\kappa_T\kappa_L}\right)^2 (R|\kappa_\perp^T|). \tag{157}$$

The fact that the entanglement contribution is negative should not disturb the reader; only the sum in Eq. (154) needs to be positive.

We obtained the results for the hydrodynamic model using $\tau\to\infty$, the dispersion relation given implicitly by Eq. (108), the R value [Eq. (123)], and the expressions for κ_T^2 [Eq. (97)], κ_L^2 [Eq. (101)], $|\kappa_\perp^T|$ [Eq. (99)], and $|\kappa_\perp^L|$ [Eq. (103)]. The numerical data for $M_>^T$, $M_>^L$, and $M_>^{TL}$ given as functions of $q_\parallel$ are shown for the three branches in Figs. 11–13, respectively.

In the major part of the $q_\parallel$ range plotted, a fairly good approximation is obtained by the simple asymptotic ($q_\parallel\to\infty$) expressions for the masses. Thus setting $|\kappa_\perp^T|\approx q_\parallel$ and $|\kappa_\perp^L|\approx q_\parallel$ and using the abbreviation

$$\mathcal{N}(q_\parallel) = \left(\frac{\mu_0\omega(q_\parallel)c^2}{2}\right)^2 q_\parallel\left[\omega^2(q_\parallel)-\omega_p^2\right]^{-2}, \tag{158}$$

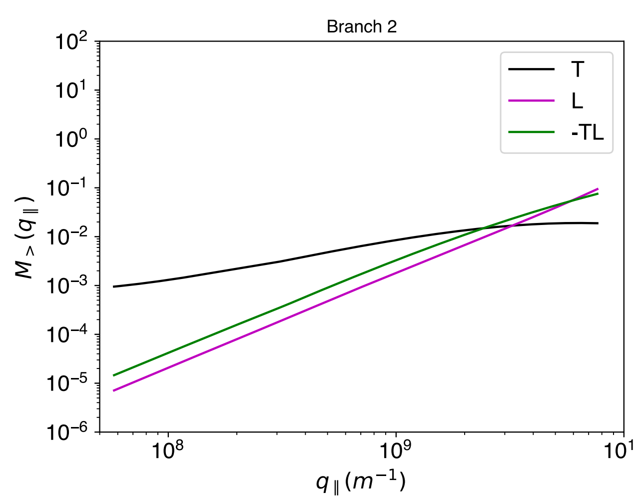

FIG. 12. Branch 2 (thick line in Fig. 3): Individual T, L, and TL jellium equivalent mass contributions as functions of the wave number $q_\parallel$. Here $-M_>^{TL}(q_\parallel)$ is plotted for the negative-TL part.

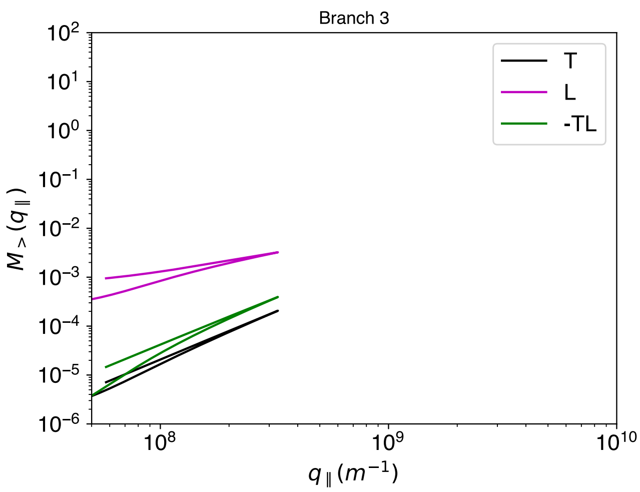

FIG. 13. Branch 3 (dashed line in Fig. 3): Individual T, L, and TL jellium equivalent mass contributions as functions of the wave number $q_\parallel$. Here $-M_>^{TL}(q_\parallel)$ is plotted for the negative-TL part. The branch only exists for wave numbers smaller than $q_\parallel \approx 3.3\times10^8$ m^{-1}.

one obtains

$$M_>^T(q_\parallel) = \mathcal{N}(q_\parallel), \tag{159}$$

$$M_>^L(q_\parallel) = \mathcal{N}(q_\parallel)\left(\frac{\omega_p}{\omega(q_\parallel)}\right)^4, \tag{160}$$

$$M_>^{TL}(q_\parallel) = -2\mathcal{N}(q_\parallel)\left(\frac{\omega_p}{\omega(q_\parallel)}\right)^2. \tag{161}$$

Note that the magnetic contribution to $M_>^T(q_\parallel)$ vanishes for $q_\parallel \to \infty$. The total equivalent mass hence takes the asymptotic form

$$M_>(q_\parallel) = \left(\frac{1}{2\varepsilon_0}\right)^2 \frac{q_\parallel}{\omega^2(q_\parallel)}, \quad q_\parallel \to \infty. \tag{162}$$

We know from the analysis in Sec. VI A that the dispersion relation of branch 1 at high-$q_\parallel$ values approaches the linear Ritchie result $\omega(q_\parallel) \approx D^{1/2}q_\parallel$ [Eq. (107) for $\tau \to \infty$]. However, this electrostatic form does not imply that the surface jellion mass can be calculated keeping only its L part. If this were the case, a resonance would occur in $M_>(q_\parallel)$ at a $q_\parallel$ value corresponding to $\omega(q_\parallel) = \omega_p$ [see Eq. (160)]. The numerical result for branch 1, presented in Fig. 10, exhibits no resonance at this $q_\parallel$ value. It appears from Fig. 11 that the equivalent mass contributions from the T, L, and TL parts all are at resonance at $\omega(q_\parallel) = \omega_p$, but the asymptotic ($q_\parallel \to \infty$) analysis leading to Eq. (162) shows that a delicate balance between the three parts occurs.

IX. SUMMARY

In this work the Weyl representation of wave fields has been used to establish the eigenmode structure of collective jellium excitations at a sharp and flat jellium-vacuum interface. The eigenmodes, which we have named surface jellions, form a complete set and are the true eigenmodes related to surface excitation spectra, emerging in optical reflection studies and when a charged particle penetrates a jellium, for instance. The $q_\parallel$ wave-number spectrum of the surface jellions includes interface entangled plasmon-plasmariton states not present in previous analysis based on the surface plasmon (L) and surface plasmariton (T) eigenmodes and their mere interference. In a manifest manner the entanglement results, in a hydrodynamic approach, in the presence of three branches in the surface jellion dispersion relation $\omega = \omega(q_\parallel)$. Outside the effective $q_\parallel$ range of entanglement, the branches of the dispersion relation collapse asymptotically into two. In an inverse dispersion relation plot $q_\parallel = q_\parallel(\omega)$, asymptotically (i.e., for $\omega/\omega_p \to 0$ and $\omega/\omega_p \to \infty$) the two branches are recognized as those belonging to surface plasmaritons [with their forbidden gap in the frequency range ω_p^s ($\equiv\omega_p/\sqrt{2} < \omega < \omega_p$)] and to surface plasmons (existing only for $\omega > \omega_p^s$).

It is known from previous studies on surface plasmaritons that the boundary (jump) conditions play a crucial role in the form of the dispersion relation in regions where spatial dispersion is important. For so-called active boundary conditions real surface currents are present. These may originate in, for example, selvedge effects or the effect of a mesoscopic (quantum-well) layer deposited on the surface. For the SCIB model passive boundary conditions (no real surface currents) can be employed. In the screened propagator formalism, here described in the Weyl expansion, some kind of surface current density distribution is needed to obtain an electromagnetic field in the jellium and vacuum half spaces. In the framework of the SCIB model, the needed sheet current density is a fictitious one directed parallel to the $\mathbf{q}_\parallel$ direction for p-polarized fields.

We illustrated the main principles of the surface jellion formalism by applying our theory in numerical calculations based on the well-known hydrodynamic model for the electron response to the prevailing field. In particular, surface jellion dispersion relations with three branches were calculated for a finite relaxation time τ and in the limit $\tau \to \infty$ (eigenmode spectrum).

Surface jellions in which the vacuum and T and L parts all decay exponentially away from the interface are nonradiative and of utmost importance as one knows from surface plasmariton and surface plasmon studies. For the hydrodynamic model, we identified the part of the ω-$q_\parallel$ domain in which the surface jellion eigenmodes are exponentially confined.

For these so-called confined surface jellion eigenmodes, we have carried out a general calculation of the associated electromagnetic momentum flow, which always is directed parallel to $\mathbf{q}_\parallel$. We illustrated the main results in a numerical study of the momentum flow for the hydrodynamic model. For each of the three branches the momentum was calculated as a function of the wave number $\mathbf{P} = \mathbf{P}(q_\parallel)$. In the major part of the studied $q_\parallel$ range, the momentum flow is opposite to $\mathbf{q}_\parallel$ inside the jellium. To this electromagnetic momentum backflow one must add the momentum carried in vacuum. The sum of these two parts is in the $\mathbf{q}_\parallel$ direction, as expected. For a coupled particle (electron)-field spectrum the total momentum is the sum of the field part and the part carried by the induced kinetic energy of the particles. The effect stemming from the particle potential energy is included in the L dynamics of the electromagnetic field.

We finished our theory with a study of the field energy associated with the surface jellion eigenmodes. By introducing a certain equivalent mass concept related to the eigenmode energy, a harmonic-oscillator description was established. This description led, via the introduction of a set of canonical coordinate and velocity variables, to a Hamiltonian formalism. Upon extension of the variables to the operator level we obtained, as expected, the surface jellion quantum energy $\hbar\omega_b(q_\parallel)$ for branch number b ($b = 1, 2, 3$). Numerical calculations of the electromagnetic equivalent mass as a function of the wave number along the surface, i.e., $M = M(q_\parallel)$, were carried out in the framework of the hydrodynamic model for each of the three branches of the dispersion relation. The mass $M = M_< + M_>$ is the sum of a vacuum part $M_<$ and a jellium part $M_>$. The mass is composed of three parts: (i) a plasmariton part M^T, which has contributions from both the vacuum and the jellium half spaces $M^T = M^T_< + M^T_>$, (ii) a plasmon part $M^L = M^L_>$, to which only the jellium contributes since there is no longitudinal field in vacuum, and (iii) an entangled TL part $M^{TL} = M^{TL}_>$. In order to obtain further insight into the structure underlying $M_>(q_\parallel)$, numerical data were presented for $M^T_>(q_\parallel)$, $M^L_>(q_\parallel)$, and $M^{TL}_>(q_\parallel)$ for each of the three branches.

A. Terminology

Over the years researchers have used various names for the collective eigenmodes of a metal (jellium). The name bulk plasmon, which refers to the rotation-free [in wave-vector space longitudinal (L)] eigenmodes, is used universally (see, e.g., Refs. [2–4,6–8,27]) and so is its related surface mode, the surface plasmon. The divergence-free [in wave-vector space transverse (T)] bulk eigenmode is most often called a bulk polariton in the literature. This name is used as reference to the fact that an electromagnetic wave traveling through a metal induces (microscopic) polarizations in the ionic lattice structure. In the jellium approximation, where the ionic potential is smeared uniformly in space, we prefer the name bulk plasmariton, a name dating back to at least Patel and Slusher [31] and used in our previous work on collective jellium excitations [15,32]. The related surface modes go under the name surface polaritons or equivalently surface plasmaritons. While authors may use either the polariton or plasmariton terminology, we warn against use of words like plasmon polaritons (surface plasmon polaritons) for the collective T modes, because these names mix in terms that refer to an L mode and hence might be confusing for the reader.

The entangled plasmon-plasmariton modes which appear in the Weyl expansion, and are studied in this paper, are genuinely new eigenmodes. Following a naming made in Ref. [17], we suggest that the names jellion and surface jellion might be used to classify the quanta of these new modes.

B. Key results

In brief, we would like to emphasize that the presence of a surface or interface inevitably leads to a fundamental entanglement between the surface plasmon and surface plasmariton modes in collective jellium electrodynamics. One important manifestation of this entanglement appears in the form of a new (third) branch of the surface (jellion) mode's dispersion relation. Outside the wave-number region of strong entanglement the three branches collapse into two in a manner which most easily is determined making use of the Weyl expansion sometimes used in rigorous diffraction analyses from, e.g., nanosize holes in a metal screen and often in macroscopic diffraction theory. By introduction of a so-called equivalent mass concept, we have shown how the quantization of the surface jellion eigenmodes can be done.

A number of numerical calculations have been carried out within the framework of the hydrodynamic approximation and we believe that the obtained entangled surface plasmon-plasmariton dispersion relations are within experimental reach using, for instance, near-field optical methods and/or inelastic diffraction techniques.

APPENDIX A: RESIDUE CALCULATION OF THE COLLECTIVE MODE PART OF $\mathbf{G}(\mathbf{q}_\parallel, \omega; Z)$

In the Weyl expansion the screened propagator is given by the integral expression

$$\mathbf{G}(\mathbf{q}_\parallel, \omega; Z) = \int_{-\infty}^{\infty} \mathbf{G}(\mathbf{q}, \omega) e^{iq_\perp Z} \frac{dq_\perp}{2\pi} = \mathbf{G}_T(\mathbf{q}_\parallel, \omega; Z) + \mathbf{G}_L(\mathbf{q}_\parallel, \omega; Z), \tag{A1}$$

where [see Eqs. (15) and (17)]

$$\mathbf{G}_T(\mathbf{q}_\parallel, \omega; Z) = \int_{-\infty}^{\infty} \frac{1}{N_T[(q_\parallel^2 + q_\perp^2)^{1/2}, \omega]} \times \left[\mathbf{U} - \frac{(\mathbf{q}_\parallel + q_\perp \hat{\mathbf{z}})(\mathbf{q}_\parallel + q_\perp \hat{\mathbf{z}})}{q_\parallel^2 + q_\perp^2}\right] e^{iq_\perp Z} \frac{dq_\perp}{2\pi} \tag{A2}$$

and

$$\mathbf{G}_L(\mathbf{q}_\parallel, \omega; Z) = \int_{-\infty}^{\infty} \frac{1}{N_L[(q_\parallel^2 + q_\perp^2)^{1/2}, \omega]} \times \frac{(\mathbf{q}_\parallel + q_\perp \hat{\mathbf{z}})(\mathbf{q}_\parallel + q_\perp \hat{\mathbf{z}})}{q_\parallel^2 + q_\perp^2} e^{iq_\perp Z} \frac{dq_\perp}{2\pi}. \tag{A3}$$

Physically, the integrals in Eqs. (21) and (22) have contributions from collective as well as single-particle excitations. The single-particle contributions are hidden in the branch cut structure of the integrands and often have been studied on the basis of the Lindhard dielectric theory in linear electrodynamics [33,34] and on the basis of the Boltzmann equation in nonlinear acousto-optic scattering [35]. Below we will be interested only in the transverse and longitudinal collective excitations. These are associated with the pole parts of the $\mathbf{G}_T$ and $\mathbf{G}_L$ integrals, respectively. Before showing how collective-mode parts of the propagator are obtained by residue calculations, let us note that

$$\hat{\mathbf{q}} = \frac{\mathbf{q}_\parallel + q_\perp \hat{\mathbf{z}}}{(q_\parallel^2 + q_\perp^2)^{1/2}} \tag{A4}$$

is a unit wave vector $\hat{\mathbf{q}} = \mathbf{q}/q$. The solutions to the dispersion relations (18) and (19), denoted by $\kappa_\perp^T$ and $\kappa_\perp^L$, are in general complex quantities. Associated transverse and longitudinal complex unit vectors defined by

$$\hat{\mathbf{Q}}_\pm^T \equiv \frac{\mathbf{q}_\parallel \pm \kappa_\perp^T \hat{\mathbf{z}}}{[q_\parallel^2 + (\kappa_\perp^T)^2]^{1/2}}, \tag{A5}$$

$$\hat{\mathbf{Q}}_\pm^L \equiv \frac{\mathbf{q}_\parallel \pm \kappa_\perp^L \hat{\mathbf{z}}}{[q_\parallel^2 + (\kappa_\perp^L)^2]^{1/2}} \tag{A6}$$

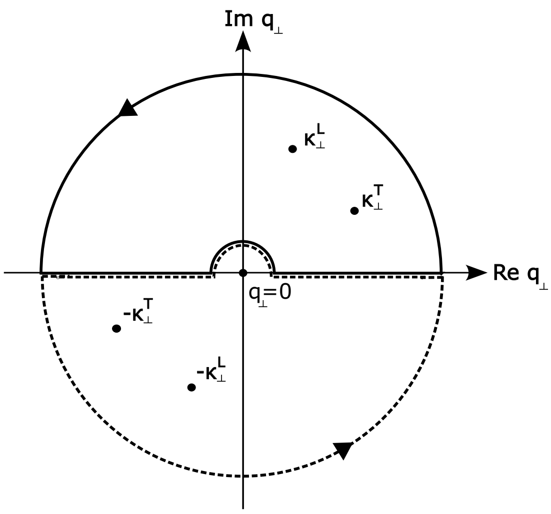

FIG. 14. Contours in the upper half plane ($\mathrm{Im}q_\perp \geqslant 0$) of a complex $q_\perp$ plane used to calculate the first-order residues $\mathcal{R}_T^{(+)}(q_\parallel,\omega)$ and $\mathcal{R}_L^{(+)}(q_\parallel,\omega)$ located at the zero points $\kappa_\perp^T$ and $\kappa_\perp^L$ for $N_T(q_\parallel,q_\perp,\omega)$ and $N_L(q_\parallel,q_\perp,\omega)$, respectively. The contour runs along the $\mathrm{Re}q_\perp$ axis (with an infinite small radius semicircle around the origin added in the $\mathcal{R}_L^{(+)}$ calculation to avoid the pole at $q_\perp=0$). In both cases, the contours are closed by a semicircle with a radius expanding towards infinity. The residues $\mathcal{R}_T^{(-)}(q_\parallel,\omega) = -\mathcal{R}_T^{(+)}(q_\parallel,\omega)$ and $\mathcal{R}_L^{(-)}(q_\parallel,\omega) = -\mathcal{R}_L^{(+)}(q_\parallel,\omega)$, located at $-\kappa_\perp^T$ and $-\kappa_\perp^L$, respectively, can be obtained using the dashed-line contour shown, again with the infinitesimal radius included in the L calculation.

are of primary importance for the residue calculation carried out.

Expanding semicircles are used as contours (and for the $\mathcal{R}_L^{(+)}$ calculation also an infinite small semicircle around the origin), which for $Z>0$ and $Z<0$ are located in the upper and lower half planes of a complex $q_\perp$ plane, respectively (see Fig. 14). Since ε_T and ε_L are functions alone of the squared quantities $(q_\perp^T)^2$ and $(q_\perp^L)^2$, the lower ($\mathcal{R}_{T,L}^{(-)}$) and upper ($\mathcal{R}_{T,L}^{(+)}$) half-plane residues, related to the poles at $\mp\kappa_\perp^T$ and $\mp\kappa_\perp^L$, satisfy

$$\mathcal{R}_{T,L}^{(-)} = -\mathcal{R}_{T,L}^{(+)}. \tag{A7}$$

As a result of the first-order residue calculations, one obtains the expressions given in Eqs. (21) and (22) for the collective-mode approximation to the screened propagator in the Weyl expansion.

APPENDIX B: CALCULATION OF ‖E‖ AND ‖B‖

It appears from Eqs. (23) and (24) that the electric field from the current density sheet is given by

$$\mathbf{E}(z) = -i\mu_0\omega\mathbf{G}(z-z_0)\cdot\mathbf{J}_0^{\mathrm{ext}}, \tag{B1}$$

omitting the reference to $(\mathbf{q}_\parallel,\omega)$ from the various arguments. The jump in the electric field across the sheet hence becomes

$$\|E\| = -i\mu_0\omega[\mathbf{G}(z\to z_0^+) - \mathbf{G}(z\to z_0^-)]\cdot\mathbf{J}_0^{\mathrm{ext}}. \tag{B2}$$

The jump in the propagator is obtained utilizing the forms given in Eqs. (21) and (22):

$$\begin{aligned}&\mathbf{G}(z\to z_0^+) - \mathbf{G}(z\to z_0^-)\\ &\quad= i\mathcal{R}_T^{(+)}(\hat{\mathbf{Q}}_-^T\hat{\mathbf{Q}}_-^T - \hat{\mathbf{Q}}_+^T\hat{\mathbf{Q}}_+^T) + i\mathcal{R}_L^{(+)}(\hat{\mathbf{Q}}_+^L\hat{\mathbf{Q}}_+^L - \hat{\mathbf{Q}}_-^L\hat{\mathbf{Q}}_-^L).\end{aligned} \tag{B3}$$

By inserting the expressions for $\hat{\mathbf{Q}}_\pm^T$ and $\hat{\mathbf{Q}}_\pm^L$ [Eqs. (A5) and (A6)] one obtains

$$\begin{aligned}&\mathbf{G}(z\to z_0^+) - \mathbf{G}(z\to z_0^-)\\ &\quad= 2iq_\parallel\left(\frac{\mathcal{R}_L^{(+)}\kappa_\perp^L}{\kappa_L^2} - \frac{\mathcal{R}_T^{(+)}\kappa_\perp^T}{\kappa_T^2}\right)(\hat{\mathbf{q}}_\parallel\hat{\mathbf{z}} + \hat{\mathbf{z}}\hat{\mathbf{q}}_\parallel).\end{aligned} \tag{B4}$$

With this expression for the jump in the propagator, the jump in the electric field [Eq. (B2)] takes the form cited in Eq. (29).

In order to derive the jump in the magnetic field, it is useful to let $\mathbf{q}_\parallel = q_\parallel\hat{\mathbf{x}}$. This implies that $\mathbf{J}_0^{\mathrm{ext}} = J_{0,x}^{\mathrm{ext}}\hat{\mathbf{x}} + J_{0,z}^{\mathrm{ext}}\hat{\mathbf{z}}$. For $z>z_0$, the transverse part of propagator (with a superscript $>$) hence is given by

$$\mathbf{G}_T^>(z) = \frac{i\mathcal{R}_T^{(+)}}{\kappa_T^2}\begin{pmatrix}(\kappa_\perp^T)^2 & 0 & -q_\parallel\kappa_\perp^T\\ 0 & \kappa_T^2 & 0\\ -q_\parallel\kappa_\perp^T & 0 & q_\parallel^2\end{pmatrix}e^{i\kappa_\perp^T(z-z_0)}. \tag{B5}$$

The related transverse part of the electric field thus has the components

$$E_{T,x}^>(z) = \mu_0\omega\frac{\kappa_\perp^T}{\kappa_T^2}\mathcal{R}_T^{(+)}\big(\kappa_\perp^T J_{0,x}^{\mathrm{ext}} - q_\parallel J_{0,z}^{\mathrm{ext}}\big)e^{i\kappa_\perp^T(z-z_0)}, \tag{B6}$$

$$E_{T,z}^>(z) = \mu_0\omega\frac{q_\parallel}{\kappa_T^2}\mathcal{R}_T^{(+)}\big(-\kappa_\perp^T J_{0,x}^{\mathrm{ext}} + q_\parallel J_{0,z}^{\mathrm{ext}}\big)e^{i\kappa_\perp^T(z-z_0)}. \tag{B7}$$

It follows from the Maxwell equation $\nabla\times\mathbf{E} = i\omega\mathbf{B}$ that the magnetic field, which points in the y direction, $\mathbf{B} = \hat{\mathbf{y}}B_y$, may have its component calculated from

$$B_y(z) = \frac{1}{i\omega}\left(\frac{\partial E_{T,x}(z)}{\partial z} - iq_\parallel E_{T,z}(z)\right). \tag{B8}$$

For $z>z_0$, using Eqs. (B6) and (B7) leads to the explicit result

$$\begin{aligned}B_y^>(z) &= \frac{\mu_0}{\kappa_T^2}\mathcal{R}_T^{(+)}\big\{\kappa_\perp^T[(\kappa_\perp^T)^2 + q_\parallel^2]J_{0,x}^{\mathrm{ext}}\\ &\qquad - q_\parallel[(\kappa_\perp^T)^2 + q_\parallel^2]J_{0,z}^{\mathrm{ext}}\big\}e^{i\kappa_\perp^T(z-z_0)}\\ &= \mu_0\mathcal{R}_T^{(+)}\big(\kappa_\perp^T J_{0,x}^{\mathrm{ext}} - q_\parallel J_{0,z}^{\mathrm{ext}}\big)e^{i\kappa_\perp^T(z-z_0)}.\end{aligned} \tag{B9}$$

The magnetic field in the domain $z<z_0$ can be obtained from Eq. (B9) by making the replacement $\kappa_\perp^T \to -\kappa_\perp^T$, as the reader may see from Eqs. (21) and (A5). Thus,

$$B_y^<(z) = \mu_0\mathcal{R}_T^{(+)}\big(-\kappa_\perp^T J_{0,x}^{\mathrm{ext}} - q_\parallel J_{0,z}^{\mathrm{ext}}\big)e^{-i\kappa_\perp^T(z-z_0)}. \tag{B10}$$

The jump of the magnetic field across the current density sheet then becomes

$$\begin{aligned}\|\mathbf{B}\| &= [B_y^>(z\to z_0^+) - B_y^<(z\to z_0^-)]\hat{\mathbf{y}}\\ &= 2\mu_0\mathcal{R}_T^{(+)}\kappa_\perp^T J_{0,x}^{\mathrm{ext}}\hat{\mathbf{y}}.\end{aligned} \tag{B11}$$

Since the longitudinal (plasmon) part of the electric field has no associated magnetic field, the result in Eq. (B11) represents the entire jump in the magnetic field across the external current density sheet. To obtain $\|\mathbf{B}\|$ for an arbitrary $\hat{\mathbf{q}}_\parallel$ direction one just needs to make the replacement

$$J_{0,x}^{\text{ext}}\hat{\mathbf{y}} \Rightarrow J_{0,\parallel}^{\text{ext}}\hat{\mathbf{z}} \times \mathbf{q}_\parallel. \tag{B12}$$

APPENDIX C: CALCULATION OF $\mathcal{R}_T^{(+)}$ AND $\mathcal{R}_L^{(+)}$

In order to calculate the upper-half-space T and L residues, we take as a starting point the following result valid for a function $F(q_\perp)$ approaching a constant ($q_\perp$-independent) value $F(\infty)$ for $q_\perp \to \infty$:

$$\lim_{z\to 0}\int_0^\infty F(q_\perp)\frac{\sin(q_\perp z)}{q_\perp}dq_\perp = F(\infty)\lim_{z\to 0}\int_0^\infty \frac{\sin(q_\perp z)}{q_\perp}dq_\perp = \frac{\pi}{2}F(\infty). \tag{C1}$$

Next we assume that $F(q_\perp)$ is an even function of $q_\perp$. Then

$$\int_0^\infty F(q_\perp)\frac{\sin(q_\perp z)}{q_\perp}dq_\perp = \frac{1}{2i}\int_{-\infty}^\infty F(q_\perp)\frac{e^{iq_\perp z}}{q_\perp}dq_\perp \tag{C2}$$

and thus

$$\lim_{z\to 0}\int_{-\infty}^\infty F(q_\perp)\frac{e^{iq_\perp z}}{q_\perp}dq_\perp = \pi i F(\infty). \tag{C3}$$

1. Calculation of $\mathcal{R}_T^{(+)}$

Let us make the choice

$$F(q_\perp) \equiv F_T(q_\perp) = \frac{q_\perp^2}{N_T(q)}. \tag{C4}$$

Residue calculation along the contours shown in Fig. 14 then gives

$$\int_{-\infty}^\infty \frac{q_\perp^2}{N_T(q)}\frac{e^{iq_\perp z}}{q_\perp}dq_\perp = 2\pi i\kappa_\perp^T\mathcal{R}_T^{(+)}, \tag{C5}$$

a result which is independent of z. Since $F_T(\infty) = -1$, because $\sigma_T(q,\omega) \to 0$ for $q_\perp \to \infty$, one obtains $\lim_{q_\perp\to\infty} N_T(q) = -q_\perp^2$. Applying Eq. (C5) to the left-hand side of Eq. (C3), one ends up with the result in Eq. (73), viz.,

$$2\kappa_\perp^T\mathcal{R}_T^{(+)} = -1. \tag{C6}$$

2. Calculation of $\mathcal{R}_L^{(+)}$

The same approach as used for the calculation of $\mathcal{R}_T^{(+)}$ now is used to obtain $\mathcal{R}_L^{(+)}$, by taking

$$F(q_\perp) \equiv F_L(q_\perp) = \frac{1}{N_L(q)}. \tag{C7}$$

Since $\sigma_L(q,\omega) \to 0$ for $q_\perp \to \infty$, Eq. (9) gives $\lim_{q_\perp\to\infty} N_L(q) = (\omega/c)^2$, and thus $F_L(\infty) = (c/\omega)^2$. With first-order poles in the upper half plane at $q_\perp = \kappa_\perp^L$ and at the origin $q_\perp = 0$, contour integration along the contour shown in Fig. 14 gives

$$\int_{-\infty}^\infty \frac{1}{N_L(q)}\frac{e^{iq_\perp z}}{q_\perp}dq_\perp = 2\pi i\left(\frac{\mathcal{R}_L^{(+)}}{\kappa_\perp^L} + \frac{1}{2N_L(q_\parallel, q_\perp = 0)}\right). \tag{C8}$$

The relation in Eq. (C3), together with the connection

$$N_L(q_\parallel, q_\perp = 0) = \left(\frac{\omega}{c}\right)^2 \varepsilon_L(q_\parallel, q_\perp = 0), \tag{C9}$$

leads to

$$\left(\frac{c}{\omega}\right)^2 = \frac{2\mathcal{R}_L^{(+)}}{\kappa_\perp^L} + \left(\frac{c}{\omega}\right)^2 \varepsilon_L^{-1}(q_\parallel, \omega). \tag{C10}$$

This result is identical to the one appearing in Eq. (74).

APPENDIX D: SELVEDGE DYNAMICS

In the present work on surface jellions we have not taken into account the modifications which inevitably may be needed if the dynamics of the selvedge is included. A full account of these modifications is beyond the scope of this paper. However, let us indicate why the results obtained in this article might be useful as a starting point for surface jellion calculations with selvedge dynamics.

On the basis of the sharp-boundary solution for the electric field $\mathbf{E}^{\text{SB}}(z)$ and the related propagator $\mathbf{G}^{\text{SB}}(z, z') \equiv \mathbf{G}(z, z') \equiv \mathbf{G}_T(z - z') + \mathbf{G}_L(z - z')$ [Eqs. (21) and (22)], one may establish the integral equation for the microscopic electric field $\mathbf{E}(z)$ in the selvedge region

$$\mathbf{E}(z) = \mathbf{E}^{\text{SB}}(z) - i\mu_0\omega\int_{-\infty}^\infty \mathbf{G}^{\text{SB}}(z, z)\cdot\mathbf{J}^{\text{SE}}(z')dz', \tag{D1}$$

with a selvedge current density given by

$$\mathbf{J}^{\text{SE}}(z) = \int_{\text{SE}} \boldsymbol{\sigma}^{\text{SE}}(z, z)\cdot\mathbf{E}(z')dz', \tag{D2}$$

where

$$\boldsymbol{\sigma}^{\text{SE}}(z, z') = \boldsymbol{\sigma}(z, z') - \boldsymbol{\sigma}^{\text{SB}}(z, z'). \tag{D3}$$

The selvedge conductivity tensor $\boldsymbol{\sigma}^{\text{SE}}(z, z')$ here takes the form of the difference between the "correct" microscopic conductivity tensor $\boldsymbol{\sigma}(z, z')$ and the sharp-boundary (SCIB) conductivity tensor $\boldsymbol{\sigma}^{\text{SB}}(z, z')$ used in this article. The scheme in Eqs. (D1)–(D3) hence uses the results of this work as a first approximation to the theory of surface jellions with selvedge dynamics. The use of a Born-scheme iterative technique solution to investigate the modifications of the surface jellion dynamics is left for future work. In first order $\mathbf{E}(z) \equiv \mathbf{E}^{(1)}(z)$,

$$\mathbf{E}^{(1)}(z) = \mathbf{E}^{\text{SB}}(z) - i\mu_0\omega\int \mathbf{G}^{\text{SB}}(z, z')\cdot\boldsymbol{\sigma}^{\text{SE}}(z', z'')\cdot\mathbf{E}^{\text{SB}}(z'')dz''dz'. \tag{D4}$$

The first-order Born result given in Eq. (D4) is adequate for numerical calculations provided $\boldsymbol{\sigma}(z, z')$ is known (approximately). In line with a previous study of ours [15] on surface plasmaritons, the Lindhard dielectric function [5] may serve as a good yet simple quantum mechanical model for a first analysis.

In the present work we left out single-particle excitations from the theory. The extent to which this may be justified was examined in detail in [15] for the surface plasmariton case. The role of the single-particle excitations for entangled surface plasmon-plasmariton states is not known and is another issue left for future work.

[1] V. Gorobchenko, V. N. Kohn, and E. G. Maksimov, in *The Dielectric Function of Condensed Systems*, edited by L. V. Keldysh, D. A. Kirzhnitz, and A. A. Maradudin (North-Holland, Amsterdam, 1989).
[2] G. D. Mahan, *Many-Particle Physics*, 2nd ed. (Plenum Press, New York, 1990).
[3] A. L. Fetter and J. D. Walecka, *Quantum Theory of Many-Particle Systems* (McGraw-Hill, New York, 1971).
[4] D. Pines and P. Nozieres, *The Theory of Quantum Liquids* (Addison-Wesley, New York, 1989).
[5] J. Lindhard, K. Dan. Vidensk. Selsk. Mat. Fys. Medd. **28**, 8 (1954).
[6] F. Forstmann and R. R. Gerhardts, *Metal Optics Near the Plasma Frequency*, Springer Tracts in Modern Physics Vol. 109 (Springer, Berlin, 1986).
[7] P. M. Platzman and P. A. Wolf, *Waves and Interactions in Solid State Plasmas* (Academic Press, New York, 1983).
[8] B. B. Dasgupta and D. E. Beck, in *Electromagnetic Surface Modes*, edited by A. D. Boardman (Wiley, Chichester, 1982).
[9] F. Flores and F. Garcia-Moliner, in *Surface Excitations*, edited by V. M. Agranovich and R. Loudon (North-Holland, Amsterdam, 1984).
[10] H. Weyl, Ann. Phys. (Leipzig) **365**, 481 (1919).
[11] L. Mandel and E. Wolf, *Optical Coherence and Quantum Optics* (Cambridge University Press, Cambridge, 1995).
[12] J. Jung and O. Keller, Phys. Rev. A **98**, 053825 (2018).
[13] F. Garcia-Moliner and F. Flores, *Introduction to the Theory of Solid Surfaces* (Cambridge University Press, London, 1979).
[14] O. Keller, J. Opt. Soc. Am. B **12**, 987 (1995).
[15] J. Jung and O. Keller, Phys. Rev. A **106**, 033503 (2022).
[16] O. Keller, Phys. Rev. B **37**, 10588 (1988).
[17] O. Keller, *Fundamentals of Photon Physics* (CRC/Taylor & Francis, New York).
[18] P. J. Feibelman, Phys. Rev. B **12**, 1319 (1975).
[19] P. J. Feibelman, Phys. Rev. B **12**, 4282 (1975).
[20] P. J. Feibelman, Prog. Surf. Sci. **12**, 287 (1982).
[21] A. Bagchi, Phys. Rev. B **15**, 3060 (1977).
[22] R. G. Barrera and A. Bagchi, Phys. Rev. B **20**, 3186 (1979).
[23] T. Maniv and H. Metiu, Phys. Rev. B **22**, 4731 (1980).
[24] O. Keller, Phys. Rev. B **38**, 8041 (1988).
[25] O. Keller, Phys. Lett. A **188**, 272 (1994).
[26] J. Jung and O. Keller, Phys. Rev. A **90**, 043830 (2014).
[27] R. H. Ritchie, Prog. Theor. Phys. **29**, 607 (1963).
[28] A. Moreau, C. Ciraci, and D. R. Smith, Phys. Rev. B **87**, 045401 (2013).
[29] A. Pitelet, N. Schmitt, D. Loukrezis, C. Scheid, H. DeGersem, C. Ciraci, E. Centeno, and A. Moreau, J. Opt. Soc. Am. B **36**, 2989 (2019).
[30] O. Keller and J. H. Pedersen, in *Scattering and Diffusion*, edited by H. A. Ferwerda, SPIE Proc. Vol. 1029 (SPIE, Bellingham, 1988), p. 18.
[31] C. K. N. Patel and R. E. Slusher, Phys. Rev. Lett. **22**, 282 (1969).
[32] J. Jung and O. Keller, Phys. Rev. A **104**, 053508 (2021).
[33] B. N. J. Persson, J. Phys. C **13**, 435 (1980).
[34] P. Apell, Phys. Scr. **23**, 284 (1981).
[35] O. Keller, Phys. Rev. B **29**, 4659 (1984).